

Review

Review of Developments in Plate Heat Exchanger Heat Transfer Enhancement for Single-Phase Applications in Process Industries

Olga Arsenyeva ¹, Leonid Tovazhnyansky ², Petro Kapustenko ¹ , Jiří Jaromír Klemeš ¹ 
and Petar Sabev Varbanov ^{1,*} 

¹ Sustainable Process Integration Laboratory—SPIL, NETME Centre, Faculty of Mechanical Engineering, Brno University of Technology—VUT Brno, Technická 2896/2, 616 69 Brno, Czech Republic; arsenyeva@fme.vutbr.cz (O.A.); kapustenko@fme.vutbr.cz (P.K.)

² Department of Integrated Technologies, Processes and Apparatuses, National Technical University “Kharkiv Polytechnic Institute”, 2 Kyrpychova St., 61002 Kharkiv, Ukraine

* Correspondence: varbanov@fme.vutbr.cz

Abstract: A plate heat exchanger (PHE) is a modern, effective type of heat transfer equipment capable of increasing heat recuperation and energy efficiency. For PHEs, enhanced methods of heat transfer intensification can be further applied using the analysis and knowledge already available in the literature. A review of the main developments in the construction and exploration of PHEs and in the methods of heat transfer intensification is presented in this paper with an analysis of the main construction modifications, such as plate-and-frame, brazed and welded PHEs. The differences between these construction modifications and their influences on the thermal and hydraulic performance of PHEs are discussed. Most modern PHEs have plates with inclined corrugations on their surface that create a strong, rigid construction with multiple contact points between the plates. The methods of PHE exploration are mostly experimental studies and/or CFD modelling. The main corrugation parameters influencing PHE performance are the corrugation inclination angle in relation to the main flow direction and the corrugation aspect ratio. Optimisation of these parameters is one way to enhance PHE performance. Other methods of heat transfer enhancement, including improving the form of the plate corrugations, use of nanofluids and active methods, are considered. Future research directions are proposed, such as improving fundamental understanding, developing new corrugation shapes and optimisation methods and area and cost estimations.

Keywords: plate heat exchanger; heat transfer; pressure drop; energy efficiency; heat recuperation



Citation: Arsenyeva, O.; Tovazhnyansky, L.; Kapustenko, P.; Klemeš, J.J.; Varbanov, P.S. Review of Developments in Plate Heat Exchanger Heat Transfer Enhancement for Single-Phase Applications in Process Industries. *Energies* **2023**, *16*, 4976. <https://doi.org/10.3390/en16134976>

Academic Editors: Jian Liu, Weiyu Tang, Junye Li, Wei Li and David Kukulka

Received: 23 May 2023
Revised: 13 June 2023
Accepted: 25 June 2023
Published: 27 June 2023



Copyright: © 2023 by the authors. Licensee MDPI, Basel, Switzerland. This article is an open access article distributed under the terms and conditions of the Creative Commons Attribution (CC BY) license (<https://creativecommons.org/licenses/by/4.0/>).

1. Introduction

To satisfy the needs of the increasing population on our planet in terms of energy and rising standards of individual comfort, a steady increase in energy demand is inevitable. Even with the contemporary trend for the use of renewable energy sources, the main proportion of energy is generated from the combustion of fossil fuels. With this, significant volumes of greenhouse gases (GHGs) are generated. About 6 Gt CO₂ equivalent was generated during the year 2020 in the United States based on data from the US Environmental Protection Agency [1]. Of that amount, 89.0% was due to fossil fuel combustion in various sectors. The European Environmental Agency [2] reported a similar picture, with 77% of GHG generation in the energy sector and 9% added by the contribution of the industry. To mitigate GHG generation, the plans in the EU include a requirement to enhance the efficiency of energy usage by 32.5% by the year 2030 [2]. One of the measures enabling the fulfilment of these plans is improved recuperation of heat energy, which is possible with the wider use of efficient, compact heat exchangers in which modern methods of heat transfer intensification are implemented [3].

One of the most efficient and widely used types of compact heat exchangers in the industry is the plate heat exchanger (PHE). The construction and operation principles of PHEs are well-described in a number of books, including those dedicated to this type of heat exchanger (e.g., [4]). The total number of papers in the SCOPUS database with the words “plate heat exchanger” in the title and abstract published between the years 1956 and 2022 was 8112, with more than half (4245) in the last 10 years. As can be seen from the graph in Figure 1, the first increase in publications per year was after the energy crisis of the 1970s, and there has been huge growth in recent years. The number of papers published in 2020 was about 500, which was twice the number from 10 years ago. This shows the growing interest in research in this promising area. To analyse all this information is not easy. Review papers in the last decade included an analysis of advances in PHE at the time of publication [5], a review of heat transfer enhancement in PHEs [6] and an attempt to make such reviews more comprehensive [7]. With references in each of these reviews, including about 200 sources, many papers on PHEs remained out of their scope.

Documents by year



Figure 1. The number of publications on PHEs in the SCOPUS database.

The state-of-the-art analysis shows that important features of different types of PHE construction, design approaches and PHE applications in heat exchanger networks (HENs) are not discussed in the available review papers. The present work is an attempt to widen the analyses of developments in the field of plate heat exchangers (PHEs) presented earlier, highlighting important construction features and their influence on PHE efficiency and methods of heat transfer enhancement, discussing PHE inclusion in the optimisation of industrial HENs with improved heat recuperation and estimating modern trends and directions for further development of PHEs. In Section 2, the differences in the construction of different PHE types are discussed, as well as their influence on heat transfer enhancement in PHEs and design methods. In Section 3, the main features of the thermal and hydraulic design for PHEs of different types are summarised, and an analysis of flow structure and the CFD modelling results is presented. The methods of heat transfer intensification in PHE channels are described in Section 4. Section 5 discusses examples of PHE applications in industry, both as individual units and as elements of HENs. This is followed by concluding remarks and recommendations for future developments in relation to PHEs.

2. PHEs and Their Types of Construction

First, we describe what we understand by the term “PHE”. A PHE is a heat exchanger with a primary heat transfer surface consisting of a number of heat transfer plates fabricated by stamping or other kinds of forceful, non-intruding deformation from thin sheet material. The interesting areas of printed circuit heat exchangers, as described in [8], and microchannel heat exchangers [9] are beyond the scope of the current review.

The main features of modern PHE construction, making them energy-efficient and reliable heat exchangers under different process conditions, are [3]:

- (i) A large number of contact points between adjacent plates in the plate pack that form a strong structure capable of withstanding large differential pressures between streams in channels [10]. This allows for plates of small thicknesses down to about 0.3 mm, decreasing the consumption of costly metals and the PHE weight;
- (ii) The PHE channels with contact points for the corrugations inside have a geometrical form inducing a change in flow direction and high levels of turbulence, swirl and vortex structures. This happens even at relatively low Reynolds numbers, as shown by various researchers (see, e.g., [11]). It creates a peculiar mechanism of heat transfer enhancement with a rather smooth transition from a laminar to a turbulent flow regime;
- (iii) Heat transfer coefficients in PHEs are much higher than in traditional shell-and-tube heat exchangers, and a significantly smaller heat transfer area is required, which makes them much more compact, with smaller area needs for maintenance;
- (iv) The area of the heat transfer surface in PHEs is made of thin metal plates and requires much less material than in shell-and-tube heat exchangers. This makes it possible to achieve lower costs, even when more expensive materials are used [12];
- (v) Often, the temperature approach of the streams in PHEs can be reduced to 1 °C, which makes them useful for maximal heat recuperation in heat exchanger networks (HENs) [13];
- (vi) By adjusting the geometries of plate corrugations, the performance of PHEs can be optimised for specific process conditions [14]. This can be achieved by assembling one of the PHEs from plates with different corrugations that enable close (within an error of one plate) satisfaction of the required duty;
- (vii) The low weight of PHEs means lower costs for transport and fewer requirements for the foundation;
- (viii) The low hold-up volume of PHEs with narrow channels makes them suitable for treating dangerous or expensive fluids. Low PHE weight ensures easier control of process parameters;
- (ix) The possibility of handling multiple streams in one PHE enables the simplification of the process unit and increases its compactness;
- (x) Easy disassembly of plate-and-frame PHEs enables mechanical cleaning, rearranging and changing of a number of plates to flexibly satisfy the required changes in process requirements;
- (xi) The heat losses to surroundings in PHEs are considerably reduced, as the plates are in contact with ambient air only at their side edges.

The main disadvantages of PHEs at all stages of their development during the period of about a century since their first applications in the dairy industry are the limited range of working conditions in terms of temperature and pressure and their unreliable operation outside this range. The main elements limiting the range of plate-and-frame PHE applications are the rubber gaskets and the places of their fixation on the plates. These limitations stimulated the development of new types of PHE construction that did not use rubber gaskets to seal the PHE channels. Welded PHE (WPHE) types have been developed where the plates are welded to seal the channels, and brazed PHEs (BPHEs) have the plates brazed together at contact points using additional filler metal (fusion-bonded PHEs can also be considered as this PHE type). Nowadays, most commercially produced PHEs have corrugations inclined to the plate axis, forming channels of crisscrossing flow types between them. The main principles of heat transfer intensification in these channels remain the same in all PHE construction types. However, some features of the thermal and hydraulic design are strongly influenced by the type of PHE construction. The three main types of PHEs are described below to analyse recent developments in more detail.

2.1. Plate-and-Frame PHEs

The history of PHEs started with the plate-and-frame type. Now, it is a traditional type of construction, the main principles of which have not changed in our century (see Figure 2). However, research to improve its elements and mechanical properties is still ongoing. Examples include studies of gasket groove mechanical performance [15] and PHE structural strength [10]. Various modifications of the ports and connections have been introduced, making it possible to handle large volumes of vapour for condensation as well as evaporation duties [16]. Extensive work has also been performed on the mechanical properties of plates and the technology for their stamping. The results of such research are mostly under the possession of leading PHE manufacturing companies and are out of this paper's scope. An important note must be added about stamping technology, where the springing of metal after the stamping has to be exactly accounted for to avoid uneven depth in the corrugations in the plate field. If it is not, the thermal and hydraulic performance of the PHE will be significantly jeopardised, as, under the differential pressure between streams, the channels will not be similar and will deform against the designed parameters.

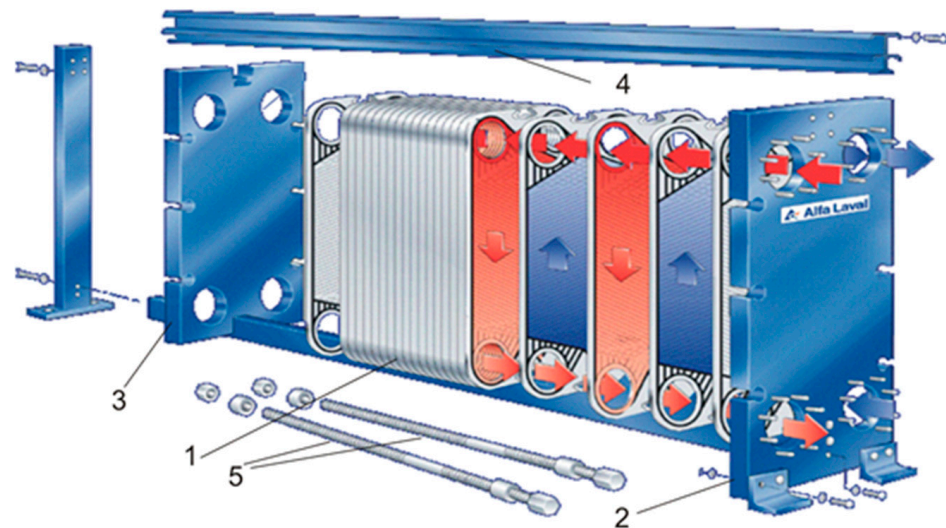


Figure 2. Plate-and-frame PHE (construction scheme): 1—stack of plates with gaskets; 2—fixed-frame plate; 3—moving plate of frame; 4—carrying bar; 5—tightening bolts (courtesy of OAO Alfa Laval Potok, Korolev, Moscow region, Russian Federation).

High temperatures, dynamic loads and contact with acids, hydrocarbons, organic solvents, ozone, steam and oxygen lead to the ageing and deformation of gaskets. A better understanding of gasket ageing can help to expand the applications of gasketed PHEs (GPHEs). The commonly used acrylonitrile-butadiene rubber (NBR) and ethylene-propylene-diene monomer (EPDM) gaskets were studied by de Souza et al. [17]. The results showed that the existence of a groove could reduce the side thermo-oxidation and that EPDM gaskets had more reliable behaviour during the experiment, where the compression in a groove was maintained for up to 360 h at 100 and 120 °C. In another paper by Zanzi et al. [18], nitrile-butadiene rubber (NBR) gaskets were investigated. The study was performed on the different geometries of gaskets, investigating the ageing under different thermo-oxidative cycles. The experiments were carried out at temperatures from 80 to 170 °C for up to 180 days. The lifetime prediction of service conditions was obtained, showing that temperature is the most influential parameter for NBR gasket ageing. Correct prediction of elastomer gaskets' behaviour would help to create the proper maintenance schedule for PHEs, reducing losses and costs.

A study of the metal bushing ring in GPHEs was carried out by Tian et al. [19], as the metal bushing ring is used for the inlet and outlet connections of the PHE and should prevent fluid leakage during operation. The authors investigated the possibility of implementing the drawing-flaring process, which consists of the deep-drawing and

multi-flaring processes forming the metal bushing rings. It can avoid the negative effects of welding seams, which can cause leakages. This paper emphasised the differences between the technologies of different manufacturers. Leading producers have not used welding seams for this element in PHEs for more than 40 years.

The details of the mechanical design of PHEs are not within the main scope of this review. Here, we present only the operational parameters of plate-and-frame GPHEs, which must be accounted for in their selection. The plates can be stamped using different metals suitable for cold stamping (commonly, the stainless steels AISI 304 and AISI 316), with thicknesses down to about 0.4 mm. More sophisticated alloys, such as alloy 254 SMO, alloy C-276, titanium, palladium-stabilized titanium, Incoloy and Hastelloy, are used for highly corrosion-aggressive media. The most limiting element of GPHEs is the elastomer gasket. The commonly used gaskets are made from nitrile rubber (NBR) and ethylene-propylene-diene rubber (EPDM) with numerous modifications. The usual temperature range of their operation is from $-45\text{ }^{\circ}\text{C}$ to $150\text{ }^{\circ}\text{C}$. New gasket materials [20] and forms [17] are being developed, and now this range can be widened to $-60\text{ }^{\circ}\text{C}$ to $200\text{ }^{\circ}\text{C}$ with more specialised gaskets. In the case of sophisticated gaskets, their cost can exceed the costs of all other elements of the PHE. The working pressure range for plate-and-frame PHEs is from vacuum conditions up to 25 bar. At high pressure, thick frame plates are required, and they can constitute most of the PHE's weight while being made from cheaper steel than the heat transfer area. Frames are produced for different pressure ranges, usually up to 10 bar, 16 bar and 25 bar, to avoid this excessive weight.

2.2. Brazed PHEs

The rubber gaskets and massive frame pressure plates are eliminated in brazed PHEs (BPHEs), which were originally developed in 1977. The adjacent plates in BPHEs are brazed at multiple contact points where their corrugations cross, as shown in Figure 3. This type of construction is capable of withstanding pressure in channels and does not need clamping by pressing the frame plates. The brazing on the plate edges seals the channels, avoiding the need for gaskets and places for their mounting. The plates are produced by stamping from a sheet of stainless steel, with thicknesses as small as 0.3 mm. Sheets of brazing metal about 0.1 mm thick are inserted between the plates to assemble the BPHE, which is finally placed in a vacuum oven to undergo thermal treatment with a specific program. Copper is most common as a brazing material, but when it is not resistant to aggressive media, such as ammonia, nickel can be used. Ni brazing filler metal has a high melting point, and additionally, Si, B and P can be added into Ni or Ni-Cr alloys to lower their melting point and improve the fluidity in their liquid state. Research on developing brazing technology with nickel is ongoing. For example, the authors of [21] presented the development of a new technology allowing the use of electrolytic Ni-P plating film as brazing filler metal with better wettability conditions, enabling reduced corrosion of the brazed area in an aqueous environment. A further advance was the creation of fusion-bonded PHEs [22], which have the same construction as BPHEs but with fusion bonding instead of brazing. This allows for completely stainless steel PHEs.

BPHEs are more compact and lower in weight than plate-and-frame PHEs. They are also cheaper in many cases. The standard operating conditions for copper-brazed BPHEs are temperatures from $-196\text{ }^{\circ}\text{C}$ to $225\text{ }^{\circ}\text{C}$ and pressure from vacuum conditions to 30 bar. For some types, the pressure can be up to 90 bar or, with special frames, up to 130 bar. Fusion-bonded PHEs (e.g., AlfaNova [22]) can operate at temperatures up to $550\text{ }^{\circ}\text{C}$. The special construction of gas-to-liquid brazed PHEs with an asymmetric "dimple" plate design can withstand gas temperatures up to $750\text{ }^{\circ}\text{C}$, with the possibility of raising the limit to $1400\text{ }^{\circ}\text{C}$ in some applications [22].

BPHEs are widely used in refrigeration, district heating, air conditioning, domestic boilers and other areas requiring low to medium heat capacities, almost entirely replacing conventional tubular heat exchangers. BPHEs can be successfully used for relatively clean fluids and where chemical cleaning is possible. The problems of fatigue can arise

in unsteady conditions and in relation to vibrations caused, for example, by reciprocating compressors or steam hammering. In such conditions, the use of BPHEs requires extreme caution.



Figure 3. Brazed PHE: (a) drawing of streams' movement; (b) example of fabricated BPHE (courtesy of OAO Alfa Laval Potok).

The main principles of the heat transfer intensification and design for BPHEs are the same as for plate-and-frame PHEs. However, the difference is the additional material at positions of plate contact points, which can change local hydrodynamics. Additionally, the absence of gaskets provides better flow conditions at the channel inlet and outlet, avoiding a decrease in the cross-section area in places where the gaskets seal the adjacent channel.

2.3. Welded PHEs

2.3.1. Welded Plate-and-Frame PHEs

The first attempt to avoid gaskets in PHEs was by welding plates in plate-and-frame PHEs. This type of PHE is very rare now, with more advanced special constructions emerging. Modifications such as semi-welded PHEs still hold their positions in a number of applications, especially in refrigeration. They consist of plate pairs welded together in twin-plate cassettes. One set of channels has only small, round gaskets; another has larger gaskets on the periphery, as in standard plate-and-frame PHEs but thicker. Such PHEs can handle aggressive fluids in one channel and, with a strong frame, withstand working pressure up to 63 bar. The significant advantage of semi-welded PHEs compared to welded ones is their much better operation with vibrations, as gaskets bring a dampening effect.

2.3.2. Welded Plate-and-Block PHEs

The most widely known and used welded PHE with plate-and-block construction is Compabloc™, schematically shown in Figure 4. It consists of a welded core, representing a heat transfer surface, encapsulated in a dismountable shell. From the view of thermal and hydraulic performance, it consists of a set of plate blocks. Each block has a cross-flow of streams. However, overall, counter-current flow exists across the whole of the PHE. From the viewpoint of thermal design, cross-flow in separate blocks causes a significant decrease in the average temperature difference in the PHE, which can be compensated by the overall counter-current flow. This depends on the required temperature program and the ratio of the two streams' heat capacities. From a hydraulic viewpoint, the construction offers good distribution across the channel width and minimal local hydraulic resistance in the channel inlet and outlet. The welded construction with a special gasket at the assembled shell allows for an extension of the working parameters, ranging from temperatures of $-46\text{ }^{\circ}\text{C}$ to $370\text{ }^{\circ}\text{C}$ at pressures from vacuum to 42 bar. The absence of gaskets not only allows for the widening of the range of working parameters but creates fatigue problems in unsteady conditions and in relation to vibrations caused, for example, by reciprocating compressors or steam hammering, which must be considered in all WPHE applications.

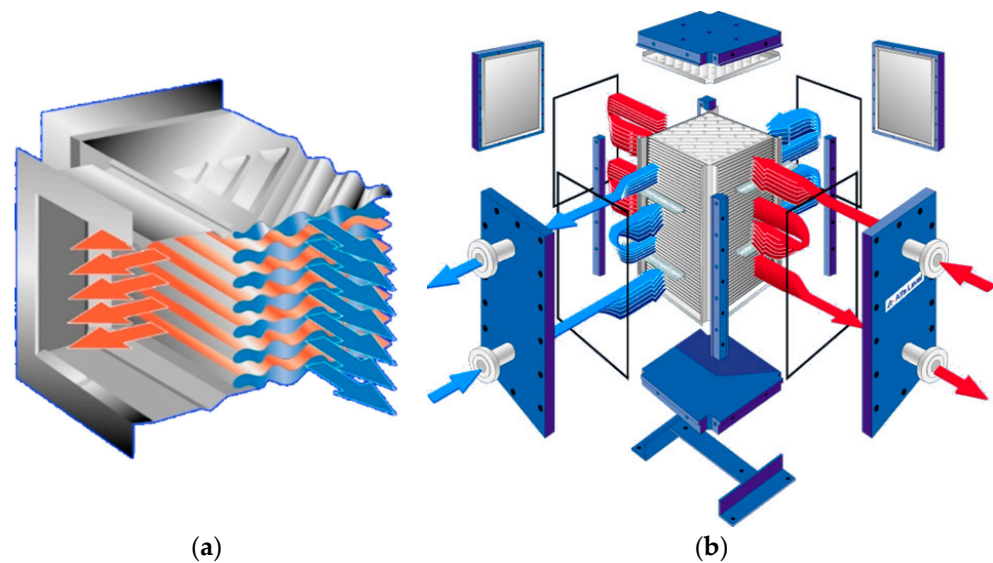


Figure 4. Compabloc™ welded PHE: (a) plate pack schematic; (b) arrangement of cross-counter-current channels for stream flow (courtesy of OAO Alfa Laval Potok).

Presently, the main PHE manufacturers produce welded PHEs with similar constructions, e.g., FunkeBlock FPB, GEABloc®, APV Hybrid-Welded Heat Exchanger, etc. [3]. The operating range of these WPHEs is close to that of Compabloc but, excluding gaskets in the shell assembly, APV Hybrid is declared to work at temperatures from $-200\text{ }^{\circ}\text{C}$ to $900\text{ }^{\circ}\text{C}$ and pressure up to 60 bar. The dismantlable shell allows access to a heat transfer surface for cleaning with a pressure water jet or repair but limits the operation range. A similar block arrangement for a WPHE employed a high-pressure shell consisting of an ammonia synthesis column [23] and could operate at a pressure of 320 bar and a temperature of $520\text{ }^{\circ}\text{C}$.

2.3.3. Welded Plate-and-Shell PHEs

Work on the shell allows the Packinox welded PHE to operate in severe conditions related to catalytic reforming and other processes in chemical and petrochemical industries. Without a separate shell reinforced by frame plates and frame, Packinox can operate at temperatures up to $400\text{ }^{\circ}\text{C}$ and pressures up to 70 bar [22]. Long corrugated plates are used in the construction with a strict counter-current flow of streams. This allows for significant improvements in heat recuperation.

Another principle for the channel arrangement is used in plate-and-shell WPHEs [24], shown in Figure 5. The pack of round plates is encased in a round shell, allowing for an arrangement with a parallel flow of streams: a counter-current in one-pass or mixed-in multi-pass PHEs. Originally developed in 1990 at Vahterus Oy, with different modifications, it can work at pressures up to 150 bar and temperatures from $-270\text{ }^{\circ}\text{C}$ to $750\text{ }^{\circ}\text{C}$ [25]. Now, WPHEs are manufactured with this principle by a number of other producers. As with all welded PHEs, they can have fatigue problems, which are investigated in, for example, [26].

Another modification of welded PHEs is the pillow-plate heat exchanger (PPHE), which consists of double-plate panels welded at multiple points and on the periphery. The panels are formed by pumping fluid at high pressure in a channel between the plates to achieve plastic deformation of the metal sheets between the welded points and to create an inside channel for the fluid flow of one stream. Being assembled in a pack, the panels form channels between them for another stream flow. The forms of the channels and their cross-sections are different, which allows the use of PPHEs for streams with very different flow rates and heat capacities, including in gas–liquid heat exchange and condensation and evaporation. The panels can be formed without expensive stamping tools. PPHEs are

not considered here in more detail. A comprehensive survey of PPHE developments and research is available in [27].

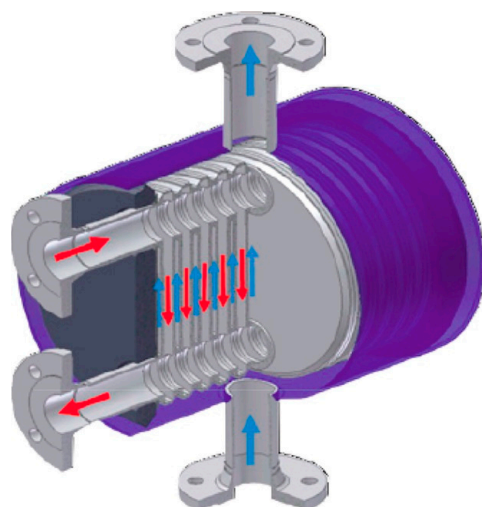


Figure 5. Schematic drawing of plate-and-shell PHE (after Freire and de Andrade [24]).

3. PHE Thermal and Hydraulic Performance

3.1. Experimental Studies on PHEs with Chevron-Type Corrugated Plates

Since PHEs were first invented, experimental investigations have been the only reliable method to obtain correlations for the thermal and hydraulic design of commercial PHEs. Even today, with fast-developing computer modelling technologies, all manufacturers' newly developed PHE plates undergo thermal and hydraulic tests to obtain the required accurate correlations for the design of PHEs with these plates. All these correlations are the property of PHE manufacturers and are included in the proprietary software for PHE design. Only those results and correlations obtained by independent researchers or with publication permission are available in the literature. Most such publications are concerned with studies on PHEs using commercially manufactured plates, as seen in Table 1. From the early days, the research has been focused on gasketed frame-and-plate heat exchangers. The most widely used are plates with inclined corrugations, which are also called chevron or herringbone plates. Schematically, such plates are shown in Figure 6. The main part of the heat transfer process between heat-exchanging streams takes place in the main corrugated field, schematically shown in Figure 7.

Table 1. Parameters from different experimental studies on PHE thermal and hydraulic performance.

Paper and Authors	Re Range	Pr Range	Geometrical Parameters	Type of PHE
Savostin and Tikhonov (1970) [28]	300 ÷ 6000	0.69 ÷ 0.72 (air)	$\beta = 72^\circ, 48^\circ, 33^\circ, 18^\circ, 14^\circ, 10^\circ$; $\gamma = 0.872 \div 0.934$, $b = 1.12 \div 1.22$ mm	Models of plate heating surface
Rosenblad and Kullendorff (1975) [29]	50 ÷ 5000	~0.7 (air, mass transfer)	$\beta = 5^\circ \div 85^\circ$	Model of PHE corrugated field
Tovazhnyanskyy et al. (1980) [30]	2000 ÷ 25,000	2.0 ÷ 8.1 (water)	$\beta = 60^\circ, 45^\circ, 30^\circ$; $\gamma = 0.556$; $b = 5.0, 7.5, 10$ mm	Models of PHE corrugated field
Focke et al. (1985) [31]	90 ÷ 50,000	No data, mass transfer	$\beta = 80^\circ, 72^\circ, 60^\circ, 45^\circ, 30^\circ$; $\gamma = 1.0$; $b = 5.0$ mm	Models of PHE corrugated field
Gaiser and Kottke (1989) [32]	2000	~0.7 (air, mass transfer)	$\beta = 12^\circ \div 71^\circ$	Model of PHE corrugated field

Table 1. Cont.

Paper and Authors	Re Range	Pr Range	Geometrical Parameters	Type of PHE
Heavner et al. (1993) [33]	550 ÷ 10,000	2.0 ÷ 8.0	$\beta = (90^\circ + 45^\circ) \times 0.5;$ $(90^\circ + 23^\circ) \times 0.5; 45^\circ; 23^\circ;$ $\gamma = 0.7$	Commercial plates
Bogaert and Bölcs (1995) [34]	10 ÷ 1000	ESSO oil: ~50	$\beta = 68^\circ; \gamma = 0.6$ b = 2.0 and 1.6 mm	BPHE
Muley et al. (1999) [35]	2 ÷ 400	130 ÷ 290	$\beta = 60^\circ; (30^\circ + 60^\circ) \times 0.5;$ $30^\circ; \gamma = 0.556$ b = 2.54 mm	Commercial plates
Muley and Manglik (1999) [36]	600 ÷ 10,000	2 ÷ 6 (water)	$\beta = 60^\circ; (30^\circ + 60^\circ) \times 0.5;$ $30^\circ; \gamma = 0.556$ b = 2.54 mm	Commercial plates
Zimmerer et al. (2002) [37]	200 ÷ 10,000	~0.7 (air, mass transfer)	$\beta = 10^\circ \div 72^\circ$	Model of PHE corrugated field
Wang et al. (2009) [38]	450 ÷ 6700	~0.7 (air)	$\beta = 30^\circ$ and 60° $\gamma = 1.0; b = 5.5$ mm	Cross-flow WPHE model
Dović et al. (2009) [39]	3 ÷ 1400	Water, water–glycerol: ~2 ÷ 100	$\beta = 65^\circ; 28^\circ$ $\gamma = 0.52$ b = 2.05 mm	Model of PHE
Khan et al. (2010) [40]	500 ÷ 2500	3.5 ÷ 6.5 (water)	$\beta = 60^\circ; (30^\circ + 60^\circ) \times 0.5;$ $30^\circ; \gamma = 0.33; 0.44; 0.54$ b = 2.2; 2.9; 3.6 mm	Commercial plates
Gherasim et al. (2011) [41]	400 ÷ 1400	~2 ÷ 6 (water)	$\beta = 60^\circ; \gamma = 0.556$ b = 2.5 mm	Commercial plates
Shaji and Das (2013) [42]	900 ÷ 7600	~2 ÷ 6 (water)	$\beta = 60^\circ; (30^\circ + 60^\circ) \times 0.5;$ $30^\circ; \gamma = 0.556$ b = 2.4 mm	Commercial plates
Kılıç and İpek (2017) [43]	600 ÷ 2250	~2 ÷ 6 (water)	$\beta = 60^\circ; 30^\circ$	Commercial plates
Kumar and Singh (2017) [44]	800 ÷ 4300	~2 ÷ 6 (water)	$\beta = 60^\circ; \gamma = 0.454$ b = 2.5 mm	Commercial plates
Yang et al. (2017) [45]	50 ÷ 500	50 ÷ 150 (oil)	$\beta = 65^\circ; 46.5^\circ; 27^\circ; \gamma = 0.571;$ 0.625 b = 2 mm, 1.25 mm	BPHEs
Khan et al. (2017) [46]	500 ÷ 2500	3.5 ÷ 6.5 (water)	$\beta = 60^\circ; (30^\circ + 60^\circ)/2; 30^\circ;$ $\gamma = 0.33; 0.44; 0.54$ b = 2.2; 2.9; 3.6 mm	Commercial plates
Panday and Singh (2022) [47]	297 ÷ 2730	~2 ÷ 6 (water)	$\beta = 60^\circ; 30^\circ; \gamma = 0.56;$ b = 3.075 mm	Commercial plates, multipass
Lee et al. (2020) [48]	~1000 ÷ 5000	~2 ÷ 6 (water)	$\beta = 65^\circ; 65^\circ + 45^\circ; 45^\circ$ $\gamma = 0.587; b = 2.2$ mm	PSPHE
Tovazhnyanskyy et al. (2020) [23]	~500 ÷ 5000	~2 ÷ 6 (water)	$\beta = 50^\circ; 40^\circ; \gamma = 0.444;$ b = 4.0 mm	Cross-flow WPHE model
Kim et al. (2021) [49]	590 ÷ 2810	~1.6 ÷ 2.0 (water)	$\beta = 45^\circ; \gamma = 0.5; b = 3.0$ mm	PSPHE
Dović et al. (2021) [11]	3 ÷ 6000	Water, water–glycerol: ~2 ÷ 100	$\beta = 65^\circ; 28^\circ$ $\gamma = 0.52$ b = 2.05 mm	Model of PHE
Beckedorff et al. (2022) [50]	3450	Water visualisation	$\beta = 75^\circ; 75^\circ + 45^\circ; 45^\circ$ $\gamma = 0.45; b = 1.95$ mm	PSPHE

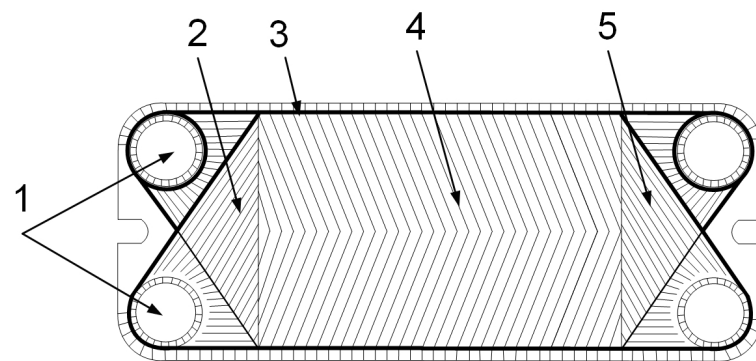


Figure 6. Schematic drawing of commercial PHE plate: 1—ports for stream flows in and out of the channel; 2 and 5—zones of flow distribution; 3—gasket; 4—the main corrugated field.

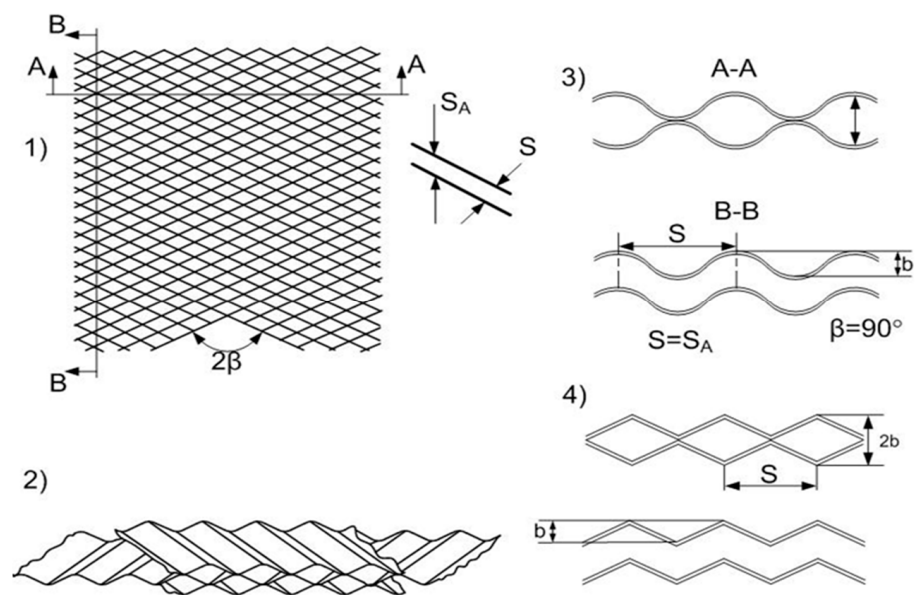


Figure 7. Schematic drawing of the main corrugated field channels: (1) corrugations crossing; (2) three-dimensional view; (3) sinusoid-shaped corrugations; (4) triangle-shaped corrugations.

The results of experiments on heat transfer and hydraulic resistance in the channels of PHEs are usually presented in the form of correlations similar to those for tubes:

$$\text{Nu} = A \cdot \text{Re}^n \cdot \text{Pr}^p \cdot \left(\frac{\mu_b}{\mu_w} \right)^m \quad (1)$$

$$\zeta = B \cdot \text{Re}^r \quad (2)$$

Here, Nu is the Nusselt number; Re is the Reynolds number; Pr is the Prandtl number; ζ is the friction factor; μ_b and μ_w are the dynamic viscosity at flow bulk and at wall temperatures, Pa·s; A, B, n, r, p and m are empirical parameters.

The values of the parameters p and m, which are powers in the components of Equation (1), are usually obtained from data previously proposed for tubes and flat channels. The power m in the viscosities ratio is usually in the range of 0.11 to 0.17 or simply omitted. The power p associated with the Prandtl number is set in the range from 0.43 to 0.3 by different researchers. The parameters B and r are usually determined by correlating with regression analysis data for pressure drops in channels. Some authors specify ζ as the Darcy friction factor and others as the Fanning friction factor, and this must be accounted for in comparisons of different authors' results. The characteristic diameter related to the Re number definition is also specified differently: as the hydraulic diameter d_h or the

equivalent diameter calculated as double the plate corrugation height b ($d_e = 2 \cdot b$). The parameters A and n are determined by correlating heat transfer data.

The empirical correlations presented by different authors are applicable only to the range of experimental conditions and geometries employed for their investigated PHE plates and channels. From all the experiments conducted by the same researchers for channels formed by plates with different corrugation geometries, starting from the paper [28], it follows that the main influencing parameter is the corrugation angle β in relation to the main flow direction. With an increase in angle β , both the heat transfer intensity (characterised by the Nu number) and friction factor increase. Most of the authors who have conducted experiments with different β angles (see Table 1) presented results by expressing their correlation parameters (A , B , n , r) as functions of β . Nevertheless, the results of calculations using equations obtained by different researchers can differ by up to 100% and more.

An attempt to generalise all the data for PHEs available at the time of publication was made in [51]. Based on theoretical flow models and empirical data from different authors, an implicit equation for predicting the Darcy friction factor was proposed that also accounted for the influence of corrugation shape. The differences in the equivalent diameter estimation by specific authors were accounted for. However, individual deviations from the mean correlation ranged from -50 to $+100\%$; e.g., the data from [52] for four BPHEs were lower, up to 30%. For the calculation of the Nu number, a special form of heat and momentum analogy (the generalised Leveque equation) was used. The Leveque equation was initially proposed for laminar flow in pipes, and its adaptation for turbulent flow in PHE channels looks rather artificial with no theoretical background. However, the deviations in most individual data values were in the range of $\pm 20\%$, with some of them up to 30%. To account for the influence of corrugation shape, the authors of [36] proposed such parameters as the corrugation profile aspect ratio $\gamma = 2b/S$ (where S is the corrugation pitch) and surface area enlargement factor ϕ (ratio of plate corrugated surface area to the area of flat, unstamped surface). In the final correlation, the parameters A and B in Equations (1) and (2) were expressed as polynomial functions of ϕ and parameters n and r as a function of angle β . It improved accuracy in prediction results for completed research, but, generally, the accuracy is not better than that of the correlation from [51]. To improve the prediction of the friction factor, the authors of [39] proposed an analytically derived equation based on the analysis of flow in the channel cell with empirically determined coefficients. It improved accuracy in the prediction of results obtained by some researchers. The individual deviations from the general correlation ranged from -47 to $+55\%$. For calculating the Nusselt number, a corrected Leveque equation was proposed, which somewhat improved the accuracy of the predictions of several researchers' results, with maximal deviations about the same as in [51].

Various published research results are generalised in [36,39,51], including experiments with PHEs assembled from commercially manufactured plates together with data for models of the PHE channel corrugated field (see Figure 7). The construction of commercial plates, the sizes of the ports and gaskets placed on them, and the flow distribution zones can vary considerably for different manufacturers and plate types. The pressure drops at the channel inlet and outlet with the distribution zones there can reach levels of up to 50% and more of the total pressure drop in the PHE, as is discussed in [14], especially with a small β angle. A generalised correlation for Darcy friction factors based on results obtained only for models of the PHE channel corrugated field was presented in [53]. It was presented in a form proposed by Churchill [54] for the friction factor in tubes, with correction of its parameters using data from [30] for models of PHE channels with corrugation angles

$\beta = 60^\circ, 45^\circ$ and 30° ; $\gamma = 0.556$; and $b = 5.0, 7.5$ and 10 mm and from [31] for $\beta = 72^\circ, 60^\circ, 45^\circ$ and 30° ; $\gamma = 1.0$; and $b = 5.0$ mm. The correlation was as shown in Equation (3):

$$\zeta = 8 \times \left[\left(\frac{12 + \frac{\pi \cdot \beta \cdot \gamma^2}{3}}{\text{Re}} \right)^{12} + \left(A + \left(\frac{37,530 \cdot \exp(-0.157 \cdot \beta)}{\text{Re}} \right)^{16} \right)^{-\frac{3}{2}} \right]^{\frac{1}{12}} \quad (3)$$

$$A = \left[p \cdot \ln \left(\frac{1 + 0.1 \cdot \beta}{\left(\frac{7}{\text{Re}} \cdot \exp \left(-\pi \cdot \frac{\beta}{180} \cdot \frac{1}{\gamma^2} \right) \right)^{0.9} + 0.27 \cdot 10^{-5}} \right) \right]^{16}$$

$$p = \left(0.061 + \left(0.69 + tg \left(\beta \cdot \frac{\pi}{180} \right) \right)^{-2.63} \right) \cdot \left(1 + (1 - \gamma) \cdot 0.9 \cdot \beta^{0.01} \right)$$

The mean squared error for the experimental prediction data from [30,31] is 6.5%. A comparison with results published in [29] shows a maximal error $\pm 20\%$ for $\beta = 72^\circ, 48^\circ, 33^\circ, 18^\circ$ and 14° ; $\gamma = 0.872 \div 0.934$; and $b = 1.12 \div 1.22$ mm. An error not higher than $\pm 20\%$ was found in comparison with the results from [39] at $\beta = 65^\circ$ and 28° with Reynolds numbers below 300. No higher error was reported in [55] in comparison with the data from [37]. This confirmed the validity of Equation (3) for the prediction of the friction factor at PHE channels' corrugated field in ranges for β from 14° to 72° , γ from 0.52 to 1.02 and Re from 5 to 25,000. A change in corrugation height with the same geometrical form from 1.12 to 10 mm does not affect the accuracy of Equation (3), in accordance with principles of similarity in hydrodynamics. The difference in corrugation shape between sinusoidal and triangular with rounded edges was also within the limits of the Equation (3) errors. A similar approach to friction factor correlation was used in [56]. In correlating data from [31], an equation was obtained predicting the friction factor with an average absolute error of 3.98%, which confirmed the usefulness of such an approach for PHE friction factor data correlation.

The local hydraulic resistances in the inlet and outlet areas of the channel have to be accounted for to calculate the pressure drop in channels of commercial PHEs with Equation (3). In [14], the coefficient of local hydraulic resistances was introduced for this purpose. The validity of such an approach was confirmed in [57] and further developed in [58].

For the thermal design of PHEs, the authors of [55] proposed a modified Reynolds analogy between heat and momentum transfer. It allows one to estimate the Nusselt number from data for the friction factor in the main corrugated field of the PHE channel determined with Equation (3) for the corrugation geometry of a considered plate. For this purpose, an equation to estimate the share of friction losses within the overall loss of pressure in the PHE channel was introduced, which was confirmed by data from CFD modelling in [59]. The accuracy of the proposed equation was verified by comparison with data from experiments on PHE channel models [28,29] and for PHEs with commercial plates [33,36,39,41,60]. The maximal deviations in the calculated Nu numbers from the experiment did not exceed $\pm 15\%$ in the following range of corrugation parameters: $\beta = 14^\circ \div 65^\circ$; $\gamma = 0.5 \div 1.5$; $\phi = 1.14 \div 1.5$. The range of Reynolds numbers was $100 \div 25,000$ and that of the Prandtl numbers was $0.7 \div 8.1$. The power factor for the Prandtl number in a correlation of the type in Equation (1) was set as 0.4.

The modified Von Karman analogy was proposed in [61] to predict heat transfer coefficients with a wider range of Prandtl numbers. An equation for the calculation of the power for the Prandtl number was proposed. It allowed us to predict Nusselt numbers using Equation (3) for the data presented in [35] with errors not larger than $\pm 12\%$ at Pr numbers from 130 to 290 and Re numbers from 80 to 400. The heat transfer data given in [34] for ESSO mineral oil were predicted with a maximal error of $\pm 2.1\%$ for $\text{Pr} \sim 50$.

3.2. CFD Modelling of Hydrodynamics and Heat Transfer in PHE Channels

With the fast development of computers and computational capacities, numerical modelling of complex flow structures is gaining momentum. Computational fluid dynamics (CFD) is capable of predicting flow structures and heat transfer with various levels of accuracy inside channels of various geometrical forms across a full range of flow regimes from laminar to turbulent, including transition areas. The most straightforward method is the integration of general time-dependent Navier–Stokes equations called direct numerical simulation (DNS). It does not require additional assumptions, but turbulent and transitional flow regimes need huge computation capacities and long times to reach the solution. For practical applications relating to turbulent flows, a number of approaches have been developed. Some of them use DNS modifications, such as large eddy simulation approaches (DNS LES), but others use Reynolds-averaged Navier–Stokes (RANS) equations with different forms of closure.

Different forms of RANS closures have been proposed. Some of them, called eddy-viscosity closures, have the form of algebraic equations. However, more advanced Reynolds-stress transport closures use solutions employing differential transport equations proposed by their authors. Among them, the two most used are the k - ϵ and k - ω models, in which one of the additional differential equations represents the turbulence kinetic energy k . The second additional equation in the k - ϵ model is for the rate of dissipation ϵ and that in the k - ω model is for the specific dissipation ω . Two of these models can be used together: a k - ω model in the near-wall region and a k - ϵ model in the outer region. This leads to the so-called SST approach. There are many ways to adjust these models' empirical coefficients, but they do not give a guarantee of the model validity with changing flow conditions.

All these approaches produce qualitatively similar but different accuracy results. In [62], eight types of RANS model closures were analysed by comparing calculation results for the same fluid in a channel with ribs perpendicular to the flow direction. The evident discrepancies between results led to the conclusion that the standard RANS closures fail to produce some flow effects at flow separation zones and differ in their values for flow velocity distributions and heat transfer intensities. The correct results could be obtained only by using strict model validation with empirical data, which does not give a guarantee for significantly different channel geometries and flow regimes. However, the models give similar qualitative flow pictures and can be used for some flow structure analyses.

The attempts at CFD modelling of flow in PHE channels of different geometries started in the 1980s with two-dimensional channels with bends in laminar and turbulent flow regimes. For example, in [63], simulations were performed using RANS equations and the k - ϵ turbulence model for a channel with right-angle bends at Re numbers from 400 to 12,000. With the development of computer capacities, the complexity of channel geometries and modelling approaches has increased. In [64], the three-dimensional flow in a unitary cell of a cross-corrugated PHE channel (see Figure 7) was considered. The CFD simulations with the RANS k - ϵ turbulence model and DNS LES were compared, and the conclusion was reached that DNS LES modelling is more precise in the prediction of friction factors and Nu numbers with ranges of Re numbers from 1000 to 7000 and corrugation angles from 30° to 75°.

Simulations with the DNS approach were reported in [65] for a 2D wavy channel and 3D cross-corrugated channel (see Figure 7) with sinusoidal corrugations inclined at 45° and different wavelengths. Three-dimensional (3D) simulations were conducted for the characteristic element of the channel with a range of Re numbers from 200 to 2000, and the correlations for the friction factor and the Nu number obtained were in good agreement with experimental results. The computing time for the 3D simulation with an IBM RS 6000 3BT workstation was about 15 h in steady-state conditions and about 350 h under non-steady conditions. This is a problem for the wider use of the DNS approach in engineering applications. A similar 3D approach for a characteristic element of a 45° cross-corrugated channel with sinusoidal corrugations and a range of Re numbers from 100 to 1000 was used in [66], with calculations for different Prandtl numbers of 0.7 and 7.

Simulations of flow in a sinusoidal wavy channel for a laminar regime and a range of Re numbers from 100 to 1000 were reported in [67] for Prandtl numbers of 5, 30 and 150. The influence of the wall corrugation aspect ratio was also investigated.

A CFD simulation of the flow and heat transfer in a unit cell of the cross-corrugated channel was reported in [68]. The calculations were conducted at Re numbers from 100 to 6000 with the use of the RANS $k-\omega$ model in a turbulent flow. The correlations for the prediction of the friction factor and Nu numbers were obtained for a corrugation angle of 45° . A detailed picture of the flow structure in a cell was presented and discussed.

Following the development of computer capacities and software for CFD simulations from the start of this century, in most research, standard CFD solvers are used. The most advanced and frequently used software tool is ANSYS [69]. In [70], ANSYS Finite Element Software with a RANS $k-\varepsilon$ turbulence model was used for the simulation of flow and heat transfer in a wavy channel with triangular bends at Re numbers from 1200 to 4000. The distribution of local heat transfer coefficients was analysed, and average Nu numbers and pressure drops were presented in comparison with experimental data. FLUENT software was used in [71] for modelling a PHE with four flat channels. The flow misdistribution between channels and inside each channel was analysed. The results were in good agreement with the experimental data.

The flow and heat transfer in a model of a PHE corrugated field was studied in [72] for Re numbers from 400 to 1400. The corrugations had a triangular form with an inclination angle of 45° , and the commercial software CFX was used to solve RANS equations with the SST turbulence model. In contrast to single-cell models, this approach allowed modelling of the flow development along the channel and its width. The friction factors and the average values of the Nu numbers were in good agreement with experimental data for a similar channel.

FLUENT software with a $k-\varepsilon$ turbulence model for the complete geometry of the PHE channel was used to study the flow misdistribution between different channels in a small PHE and the distribution of flow in a single channel [73]. The simulations were conducted with a range of Re numbers from 400 to 1300, and friction factor and Nu numbers showed good agreement with available experimental data. The simulated Nu numbers were between 3% and 18% lower than the experimental values. With the same software, the process in two channels of a PHE with commercial plates was simulated in [74]. The corrugation angle in the heat transfer field was 65° , and simulations performed with Re numbers from 200 to 1700 showed good agreement for the calculated friction factors and Nu numbers with experiments with this range of Re numbers.

With the further development of CFD simulation software, the modelling of flow structure and heat transfer in PHE channels with different complex geometries has become more available to engineers without advanced knowledge of numerical methods and turbulence modelling problems. This has allowed them to consider more complex problems of engineering interest. In [75], the influences of various forms of corrugation profiles on the friction factor and heat transfer were studied. Flow modelling in a unitary cell was used. The entrance effects were discussed, and the model was validated with experimental data available in the literature for traditional corrugation shapes. The correlations for friction factors and Nu numbers were presented. After analysis, the authors concluded that a sinusoidal shape for corrugations is the best, accounting for the technology of the manufacturing.

In [59], simulations were performed for a model of a PHE channel corrugated field, with model validation undertaken using experimental data for a channel with the same geometrical parameters. The share of friction losses contributing to the total loss of pressure and the distribution of shear stress on the wall of the plates with triangular corrugations were obtained. The effect of the corrugation inclination angle on the performance of a plate-and-frame PHE was studied in [76]. This effect was investigated for brazed PHEs using CFD modelling in [77], and correlations for the friction factor and Nu number were obtained. The influence of the corrugation depth was studied in [78]. The specific problem

of flue gas cooling by air in PHEs was considered in [79], and correlations for Nu number calculations in different channels were obtained.

All those papers [59,75–79] used flow models based on averaging NS equations with the use of turbulence models, mainly the k - ϵ model. These models have empirical constants that can be adjusted for the considered flow, hence limiting model validity for other cases with different channel geometries and other Re numbers and fluid properties. The DNS LES approach has fewer such empirical parameters and can be expected to be more robust with proper selection of eddy filtering. DNS LES modelling was used in [80] in an investigation of flow structure and heat transfer in brazed PHEs with different corrugations angles. This method was also used in [81] for modelling the corrugation angle's influence on the friction factor in PHE channels. It was noted that the DNS LES method could also be applied to laminar flows to obtain solutions with a wide range of Re numbers. The comparison with the experimental results from [31] showed good accuracy at angles of 60° but lower accuracy at 30° , with discrepancies of about 30%. The correlation for friction factor estimation with different corrugation inclination angles was presented.

The widespread application of brazed PHEs in refrigeration, the communal sector and other industries encouraged interest in CFD modelling of the fluid flow and heat transfer in their channels. The distribution of flow among the channels of a BPHE was studied in [82]. Two models were used for the simulation of the pressure distribution in the BPHE headers: the 3D CFD model and the simpler 1D model proposed by the authors. The validity of both models was confirmed by comparison with experimental data. While the 3D CFD model had slightly higher accuracy, the 1D model had the advantage of simplicity and is easier to use in engineering applications. A CFD study of the flow and heat transfer in channels of a brazed PHE with different corrugation angles, including mixed arrangements, was performed in [83]. The correlations for the friction factor and Nu number calculations in such channels were proposed. The modelling of flow and heat transfer in a BPHE with plates corrugated at 75° was reported in [84], where the correlations for the friction factor and Nu numbers were presented.

The CFD modelling of flow in a cross-flow heat exchanger with plates corrugated at 45° was reported in [85]. The RANS k - ω SST model was used. A special procedure was applied to adjust model constants according to the experimental data obtained by the authors with an experimental rig described in the paper to improve the model accuracy. As a result, the correlations for the Euler number and Nusselt number calculations were obtained. It is unclear how the cross-flow arrangement of streams is accounted for when obtaining correlations for Nu numbers. This can raise a concern about the possibility of including cross-flow correction in adjustments of turbulence model constants. It emphasises the importance of correctly accounting for all factors influencing PHE performance in any type of experiment, including numerical experiments with CFD simulations. A CFD study of convective heat transfer in a cross-flow block-type PHE with plates corrugated at 45° was reported in [86] accompanied by modelling of a plate-and-shell PHE. The realisable k - ϵ model was adopted with FLUENT software. A special procedure was applied to adjust the clearance between adjacent plates to maintain the needed mesh quality. The model was validated according to experimental data obtained by the authors with the experimental rig described in the paper. As a result, the correlations for the Colburn heat transfer j factor were obtained.

CFD simulations are a powerful tool for the study of flow structure and heat transfer in PHE channels with complicated geometries and flow distribution between channels. They can improve the understanding of heat transfer enhancement principles and help in estimating local process characteristics, as in [11]. However, they can only be considered in terms of numerical experiments with flow models. For practical applications of their results in PHE designs, most of the authors presented results in the form of correlations, which is typical for the presentation of physical experiment results.

4. Intensification of Heat Transfer in PHE Channels

The intrinsic feature of PHE channels formed from corrugated plates is the intensification of heat transfer compared to traditional tubular heat exchangers. The level of this intensification depends on the geometrical parameters of the corrugations and other construction features. Further increasing the level of heat transfer intensification while maintaining the same pressure losses in PHEs is the subject of much research. There are three main ways to achieve this goal: (i) passive enhancement through channel surface modifications; (ii) use of nanofluids as a new type of heat transfer media; and (iii) active methods of enhancement with the use of external effects. The enhancement of the overall heat transfer via fouling mitigation in PHEs is outside of this review's scope.

4.1. Passive Methods through Modification of the Channel Surface Geometry

4.1.1. Asterisk, Compound and Special Transverse Forms of Corrugations

In a number of research projects, new forms of corrugations on plate surfaces have been studied. In [87], the authors presented the results of experiments with a PHE formed of plates with a special asterisk form for the corrugations. More traditional designs with PHEs composed of flat plates and other plates forming wavy 2D channels were also studied. It was found that there was more intensive heat transfer in PHEs with the new asterisk corrugations on the plates than in the other two studied PHEs. However, no comparison with cross-corrugated chevron plates was presented. Moreover, the construction strength of such corrugation forms was not checked, and they have considerably fewer contact points compared to traditional PHEs with cross-corrugated plates. This creates doubts about the practical applications of such a plate design for commercial PHEs.

A PHE with a new compound longitudinal and transverse form for the plate corrugations was studied experimentally and with CFD simulation in [88]. The correlations for the Nu numbers and friction factor obtained with both methods are presented. The differences were not greater than 10%. The authors also compared the correlation with one of the traditional corrugation forms and noted that the performances of both were similar. The plates with the investigated form of corrugations are more expensive to manufacture but can be recommended for PHEs working with unclean working fluids inclined to flow clogging.

4.1.2. Undulated Corrugations with Surface Optimisation

In [89], the optimisation of a PHE made from plates with undulated corrugations was discussed based on the results of CFD modelling. Plates with different corrugation angles, distances between them and aspect ratios were investigated at Re numbers from 500 to 6000. Recommendations for PHE designers to use higher corrugation angles and smaller distances between plates were made, but the final choice to use the paper results as an additional tool for decision-making remains up to the designer. Multi-objective optimisation based on CFD simulations of a PHE with a sinusoidal form for the corrugations was presented in [90]. The most important geometrical parameters were determined to be the corrugation inclination angle and surface area enlargement factor, but results must be obtained for specific process conditions. No more specific recommendations were given. Parametric optimisation of the corrugation angle for a brazed PHE based on CFD modelling was undertaken in [91], and an angle of 30° was recommended for some specific water flow rates through PHEs.

4.1.3. New Forms of Plates and Corrugations for Cross-Flow and Mixed-Flow PHEs

The specific form of a double-wave corrugation for a cross-flow air-cooled PHE was studied experimentally in [92]. The double-wave PHE exhibited about 50% better heat transfer performance than the conventional PHE but with an increased pressure drop. That required the authors to recommend some modifications to the construction. The heat transfer by airflow was studied experimentally and numerically in [93] for corrugations with in-phase and anti-phase secondary corrugations. A reduction in pressure drops by

about 15% was predicted. In further research, the optimisation of this type of corrugation has been presented [94].

A new form comprising a hexagonal plate with spherical corrugations was investigated in two papers by authors from the same university. The results of the experimental and numerical studies are reported in [95] with a presentation of the correlations for Nu numbers and friction factors in ranges for Re from 1500 to 30,000 and Pr from 0.6 to 160. The use of this type of PHE for multi-media heat exchange was discussed in [96]. Another original rectangular form for a welded PHE was investigated experimentally and numerically in [97], with optimisation based on grey correlation theory. The construction itself and the method of optimisation are interesting, but some drawbacks of this approach were discussed in [98]. Another original construction of a helical-plate heat exchanger with two channels in helical form was studied experimentally in [99]. The walls of the channels were smooth with no corrugations, and the usual PHE heat transfer enhancement was not used for the obtained heat transfer coefficients that seemed lower than in PHEs with corrugated chevron plates, but an exact comparison was not presented. The modification of a PHE with flat plates was studied in [100] experimentally and by CFD simulation. The authors found increased compactness compared to a traditional flat-plate heat exchanger. Other modifications of such heat exchangers were studied in [101], and correlations for the Nu number and friction factor were presented. However, the PHE with flat channels has much lower constructional strength than the PHE with plates with inclined corrugations. It is limiting their wide application in the industry.

4.1.4. Capsule-Type and Dimpled Special Forms of Corrugations

Various new forms of corrugations have been proposed to improve the efficiency of PHEs. In [102], capsule-type corrugations were proposed and studied numerically. The correlations for the friction factor and heat transfer were obtained, but the absence of model validation requires the obtained enhancement in PHE performance to be confirmed with physical models and in practice. A PHE with plates with a special dimpled and protruded form for the corrugations was studied experimentally in [103] with air–air heat transfer. The absence of comparison with other forms of PHE plate corrugations makes it difficult to evaluate the performance enhancement. A similar conclusion can be applied to the results of another experimental study on the water–water heat exchange with a dimpled PHE [104]. However, the intensification of the heat transfer compared to channels with flat walls was confirmed.

In [105], a PHE with dimpled plates was studied experimentally using water and Al_2O_3 /water nanofluid. Intensification of the heat transfer compared to a flat channel and its further increase with the use of nanofluid was confirmed. A new plate geometry was studied with CFD modelling in [106] with a range for the Re number from 500 to 5000. The authors stated that the model was validated through comparison with the analytical solution, but this is doubtful at such Re values, which correspond to transitional and turbulent flow regimes. Therefore, a high level of heat transfer enhancement compared to other plate types still requires confirmation by physical experiments. An original form comprising a wavy 2D channel was proposed and studied with CFD modelling [107]. The authors validated their model by comparison with experiments on PHEs with cross-corrugated plates forming a 3D channel. Such validation was incorrect, not accounting for the different meanings of the corrugation angle in the compared papers. A practical way for the realisation of such a channel in industrial PHEs is not clear. Interesting results were reported in [108] for an experimental and CFD modelling study of heat transfer and pressure drop in a small PHE with a chevron corrugation pattern. The sizes and corrugations of the experimental sample were similar to those of a small BPHE. The maximal friction factor values were obtained at a corrugation angle of 30° and maximal Nu at 60° . Such deviations from the trends reported in other sources require a more detailed explanation.

4.1.5. Optimisation of Chevron-Type Corrugations

Attempts to optimise the structure parameters of a PHE using CFD modelling of the convective heat transfer in a corrugated field of one channel were reported in [109]. The optimised structure could reduce the coolant temperature by 2.5% and the pressure drop by 40%. However, the assumptions for the boundary conditions and not considering ports and collectors could lead to much larger errors. The liquid flow and heat transfer in a PHE with multi-chevron corrugated plates was studied experimentally and numerically in [110]. The complete channel, including ports, was modelled with CFD using five different turbulence models for the RANS equations. The shear stress transport (SST) k - ω model gave the best results compared to experimental data. The model was validated with experimental data at Re numbers ranging from 1200 to 5000, which confirmed the existence of a turbulent flow regime in PHE channels at these Re numbers. The turbulent flow regime in the PHE channel develops at much lower Re numbers than in tubes (down to 100), as has been shown experimentally in a number of studies; e.g., [4], where interesting results concerning flow structure and its distribution across the channel, which influenced heat transfer enhancement for the investigated corrugation form, are reported.

4.1.6. Modifications of Plate Surface with Artificial Roughness

The intensification of heat transfer in PHE channels through an increase in plate surface roughness has been studied in a number of research projects. The experimental study in [111] was performed for water–water heat exchange in a PHE with commercial plates specially treated to increase the roughness of the AISI 316 stainless steel surface by about five times compared to the original standard conditions. There were no significant differences in overall heat transfer coefficients, which were at high flow rates, and they were higher for standard commercial plates and plates with a rough surface at lower flow rates. In [112], experiments were performed for water–ethanol heat exchange with a PHE with commercial plates specially treated to increase the roughness of the AISI 316 stainless steel surface by about three times compared to the original standard conditions. The results were compared with data for a PHE with untreated plates. The heat transfer coefficients for the ethanol side were somewhat higher for the modified plate, but on the water side, they were higher for standard commercial plates. There was no distinct conclusion on the advantage of plates with increased roughness. PHEs with commercial plates with surface roughness increased by up to 3.3 times compared to standard conditions using a sandblasting machine and were studied experimentally in [113]. The heat transfer coefficients of the plates with rough surfaces increased from 4.46% to 17.95% compared to standard surface conditions, and the friction factor increased from 3.9% to 19.24%. This shows a certain increase in PHE performance. Results of experiments with similar roughness levels for commercial plates with different corrugation angles were reported in [114]. A significant influence from the plate corrugation angle on heat transfer and pressure drop of water in the PHE was observed, but the increase in the heat transfer with surface roughness was just mentioned without any quantified estimation.

The modification of a commercial plate surface from AISI 304 stainless steel by electrochemical etching and its effect on PHE performance were studied experimentally in [115]. Increases in the overall heat transfer coefficient compared to the untreated plate from 10.5% to 17.7% and film heat transfer coefficient from 15.3% to 32.5% were observed with an increase in the friction factor from 21.3% to 87.3%. For the comparison of different surfaces, the authors used performance evaluation criterion η determined by Equation (4) in analogy with the criterion used with enhanced tubes for the comparison of the heat transfer load transferred through surfaces with equal areas and the same pumping power for the heat agent, as shown in [3].

$$\eta = \left(\frac{Nu_1}{Nu_2} \right) / \left(\frac{f_1}{f_2} \right)^{0.33} \quad (4)$$

The performance evaluation criterion resulted in values for most of the data of about 1.11 and, for data published by the same authors [116] for similar modified plates, from 1.11 to 1.13. The authors of [116] reported a further increase in PHE performance with surface coatings using nickel (from 0% to 2.4%), copper (from 6.5% to 10.9%) and silver (from 7.7% to 16%). Overall, upon analysis of these six papers, it can be concluded that heat transfer enhancement through sandblasting roughness is not convincing, as data from some papers show some an increase but also a decrease in performance. Some others show just a marginal increase. For surface etching, the data are rather more certain, especially for coating with a highly heat-conductive material, such as silver. However, with such levels of intensification, an economic analysis of the proposed methods would be necessary.

4.2. Heat Transfer Enhancement through the Use of Nanofluids

The fast development of electronics, computing and communication technologies in the last decades of the last century stipulated the need for efficient microscale cooling equipment and technologies. To further increase compactness and cooling power, a special sort of liquid was introduced called nanofluid, the thermal properties of which are enhanced by the presence of nanometre-sized particles of 1–100 nm. At such sizes, particles are different from the original material and create stable suspensions with liquids. Their presence in certain small quantities can significantly increase heat conduction, enhancing heat transfer and changing other liquid properties. The successful application of nanofluids in microscale equipment has encouraged research on their use in other areas related to heat transfer, especially in PHEs, which are inherently compact and already demonstrate heat transfer enhancement in other ways.

The growing number of publications on convective heat transfer in nanofluids flowing inside PHE channels have been analysed in a number of reviews published following the start of our century. The general characteristics of nanofluids and their use in heat transfer equipment at the initial stages of these studies were discussed in [117]. Papers on heat transfer enhancement with nanofluids in PHEs published before 2015, including experimental and numerical studies, were surveyed in [118]. A similar review, including statistical analysis of papers on nanofluids in PHEs and more recent publications, was presented in [119]. A classification of nanofluids and a discussion of their properties in relation to PHE heat transfer enhancement are given in [120]. The methods for preparing nanofluids and for the numerical analysis of their flows in channels of different heat exchangers, including PHEs, are surveyed and discussed in [121]. Overall, there are extensive analyses of the published literature on heat transfer enhancement in PHEs using nanofluids, and it is not repeated here. The interested reader can find information in the specialised review papers cited above.

Heat transfer enhancement with nanofluids is a promising method with sufficiently high efficiency. In this paper, only brief notes on the application of this method for enhancing heat transfer in PHEs operating in process industries are presented. The use of nanofluids for heat transfer enhancement is limited to closed circuits of heat media in which nanofluids can be prepared and utilised without loss. This is impossible for general process streams and only possible for utility systems. However, with the large volumes of liquids in such systems, the cost of the nanomaterials needed must be accounted for. The application of nanofluids in the closed cooling circuit systems of industrial enterprises requires further research regarding their stability over long time periods. Possible sedimentation of nanoparticles and changes in their properties have to be eliminated. Possible application in district heating systems also requires further research regarding nanofluids' stability and the economic aspects of their use compared to other methods of heat transfer enhancement.

4.3. Heat Transfer Enhancement with Active Methods

Active methods of heat transfer enhancement in heat exchangers of different types include external action on the heat transfer surface or heat media through different forces created by electric fields, magnetic fields or ultrasound or mechanical interactions [122]. There is a more recent survey in [123]. Considerably fewer researchers have studied these methods compared to passive enhancement techniques, and fewer papers have been published [124]. For an application in heat storage systems, active enhancement techniques were analysed in the review in [125], and this application can be classified as a PHE for such systems. Few research works are dedicated to active enhancement methods, especially in PHEs, and most of them studied heat transfer enhancement using pulsating flow and ultrasound, as has been reviewed for applications with different heat exchanger types [126].

The results of an experimental investigation of heat transfer enhancement using pulsating flow with different frequencies in a PHE are reported in [127]. Tests were performed, including a test of the presence in water of different nanoparticles: graphene nanoplates (GNPs), multi-walled carbon nanotubes (MWCNTs) and their mixture. The results showed an increase in the Nusselt number up to 58% at the highest pulsation frequency of 30 Hz, with a volume concentration of 0.01%. However, for pure water, no increase in heat transfer was observed. The increase in the friction factor did not exceed 1%.

The influence of low-frequency vibration on heat transfer in CuO/water nanofluid in a PHE was studied in [128]. The increase in the overall heat transfer coefficient with an increase in vibration frequency from 30 Hz to 60 Hz was observed, with mitigation of the formation of fouling on the plate walls. The effects of such a heat transfer enhancement method were similar to those in tubular heat exchangers [129]. The effect of ultrasound on the formation of biofouling in a PHE was investigated in [130], and its ability to improve the corrosion resistance of plates was confirmed in [131].

Methods of heat transfer enhancement with electric and magnetic fields are very rare for PHE applications, but some may be promising, e.g., the piezoelectric fan method experimentally studied for channels in [132].

5. PHEs in Various Applications as Individual Units and in Heat Exchanger Networks

PHEs with different constructions and modifications have proved their higher performance and advantages compared to conventional shell-and-tube heat exchangers in a large number of applications. Numerous successful examples of such applications can be found on the websites of PHE manufacturers, e.g., [16,22,133]. Various examples of PHE applications have been studied and described in papers by a number of scholars. The earlier applications of PHEs (before 1980) in heat recovery systems were discussed by Lamb [134], who cited the examples of synthetic fibre factories, sulphuric acid production, a power station, a coke oven plant for benzolised oil preheating, heat recovery from flue gas and pasteurisation in the food industry. Significant savings in energy and costs were reported for all these cases. Grillot [135] reported a considerable reduction in fouling rates compared to tubular heat exchangers for a gasketed PHE at a sugar factory and for the Packinox WPHE at a petrochemical plant. An analysis of PHE performance and factors influencing it, based on about 16 examples of different successful applications in the chemical and process industries, was reported by Reppich [136]. The application of PHEs in the automotive industry was discussed by Lozano et al. [137] and in the textile industry by Kandilli and Koclu [138]. The energy efficiency of phosphoric acid production can be significantly increased with the application of PHEs [139].

By the estimation of Andersson et al. [140], in the year 2008, more than 750 Compabloc WPHEs were operating in oil refineries worldwide, including 200 for crude oil preheating. Freire and Andrade [24] suggested the possibility of PSHE applications in nuclear power, and Tovazhnyanskyy et al. [23] studied the operation of WPHEs in ammonia synthesis production at temperatures up to 520 °C and pressures of 320 bar. PHEs have become the preferential type of heat exchanger for district heating (DH) systems and refrigeration

technologies [60] and are of primary importance for the transition to new energy-efficient generations of DH [141].

The efficient performance of PHEs in many industrial processes has encouraged their use in newly developed process systems and in energy-saving retrofits of already existing factories. In these cases, PHEs must be considered as elements of the heat exchanger network (HEN) of the processing system and included in the problem of total system optimisation. A powerful tool for increasing process systems' energy efficiency is the process integration methodology [142]. It proposes a method of analysis and optimisation of heat recuperation HENs in process systems and has been proven to provide energy-efficient and economically viable results in a wide variety of applications. The use of modern compact heat exchangers, such as PHEs, can further increase the power of process integration, introducing more options for enhanced heat recuperation as a solution to the optimisation problem.

The significant increases in heat recuperation and energy usage efficiency achieved by applying process integration to a heat pump with the use of a PHE in the HEN of a cheese production factory were shown in [143]. The economic efficiency allowed a payback period for the renovation project of about 10 months. A proposed renovated HEN with PHEs for sodium hypophosphite production [144] made it possible to save about 55% of the energy consumed in the process. Process integration with the use of efficient PHEs for a carbon dioxide post-combustion capture unit HEN [145] enabled a decrease in energy consumption by 24% compared to the decrease of 11% that could be obtained with the use of shell-and-tube heat exchangers, with over 10% lower investment costs. Process integration with the use of PHEs for waste heat recovery from exhaust gas streams at tobacco factories [146] resulted in a decrease in carbon dioxide emissions by 600 t/y, with a payback period of about four months. The importance of using PHEs in the development and retrofitting of HENs for different industries was emphasised by Li et al. [147] and shown through practical examples of HEN retrofitting with a detailed PHE design in [13].

6. Conclusions

This article reviews the development trends and the state-of-the-art for heat transfer enhancement with PHEs. The presented survey and analysis of the literature reveal that PHEs are currently a well-established and efficient type of heat transfer equipment for process industries. The development of the channel sealing and plate forms of PHE modification makes it possible to use them in practically all types of applications in process industries. The main modifications are plate-and-frame PHEs, welded PHEs (WPHEs), brazed PHEs (BPHEs) and plate-and-shell PHEs (PSPHEs). In the majority of modern PHEs, plates with inclined corrugations are used that are assembled in packs with strong, rigid construction and multiple contact points between adjacent plates.

The channels between the PHE plates have complicated crisscrossing flow forms for the movement of heat-exchanging streams. The geometry of these channels stimulates high levels of turbulence and an increase in heat transfer intensity. The transition of flow from laminar to transitional and turbulent regimes takes place at much lower Reynolds numbers than in flat-wall channels and tubes.

Experimental research is the main method of obtaining reliable correlations for heat transfer and friction factor calculations for PHE channels. The results of numerous research studies show that the main factor affecting PHE heat transfer and hydraulic performance is the angle of the corrugations on the plates in relation to the main flow direction. The Nusselt numbers in PHE channels are larger than in flat-wall channels. At the angle of 30°, Nu is about two times larger, and a further increase in this angle from 30° to 60° increases the Nu number up to two times more, depending on the Re number. The variations in the research results depend on the tested experimental plate construction. Friction factors obtained with different models of PHE channel corrugated fields are generalised by one correlation. Accounting for the processes in the corrugated field and at the inlet and outlet

of the PHE channel separately allows adequate modelling of the heat transfer and pressure losses in the PHE.

CFD simulation is a powerful tool for investigating hydrodynamics and convective heat transfer in PHE channels with complex geometries. It allows us to obtain a detailed qualitative picture of the process of hydrodynamics and the mechanism of heat transfer intensification. However, the method is similar to experimental investigations and can be called a numerical experiment. In most papers, to obtain results useful for PHE design, correlations of the same form as in physical experiments are obtained. The difference is that the CFD models must be properly quantitatively validated, and the validation with one set of conditions does not guarantee validity in different conditions, and results must be used with caution.

To further increase heat transfer intensification, the methods developed for other types of heat exchangers can be used. The most promising applications in process industries are passive methods of heat transfer enhancement using modifications of PHE plate corrugations and channel geometries. Among them are the methods of corrugation parameter optimisation. The use of unstructured surface roughness created with sandblasting does not look like a prospective method for single-phase heat transfer, but other methods of creating small-scale surface modifications may be promising. The use of nanofluids as heat transfer media can considerably enhance heat transfer in PHEs, but the application of this method in process industries is limited to utility systems with closed circuits of heat media. The economic aspects of such enhancement must be considered. Active methods for heat transfer enhancement in PHEs are rare.

This analysis of the reviewed publications allows the authors to recommend the following areas of future research. (I) Improvement of the understanding of the fundamental principles of single-phase heat transfer enhancement in the channels of PHEs with inclined corrugated plates. (II) Investigations of new corrugation shapes experimentally and with CFD modelling with the aim of heat transfer enhancement. (III) Development of methods for optimisation of PHE plates and their corrugation geometries for operation in specified process conditions. (IV) Research on the use of nanofluids for heat transfer enhancement in PHEs and their combination with active ultrasound methods. (V) Development of methods for PHE area and cost estimation in solving HEN optimisation problems.

Author Contributions: Conceptualization, J.J.K. and L.T.; methodology, O.A. and P.S.V.; validation, P.K., O.A. and P.S.V.; formal analysis, P.K.; investigation, O.A.; resources, J.J.K.; data curation, L.T.; writing—original draft preparation, P.K.; writing—review and editing, J.J.K. and P.S.V.; supervision, L.T.; project administration, P.S.V.; funding acquisition, J.J.K. All authors have read and agreed to the published version of the manuscript.

Funding: This research was funded by European Commission and is a part of the HORIZON 2020 project RESHeat H2020-LC-SC3-EE-2020-1 on the basis of grant agreement no. 956255 and the OP VVV project “International mobility of researchers of the University of Technology in Brno II”, reg. no. CZ.02.2.69/0.0/0.0/18_053/0016962 (MeMoV II).

Data Availability Statement: Not applicable.

Conflicts of Interest: The authors declare no conflict of interest. The funders had no role in the design of the study; in the collection, analyses, or interpretation of data; in the writing of the manuscript; or in the decision to publish the results.

References

1. United States Environmental Protection Agency. Sources of Greenhouse Gas Emissions. 2022. Available online: <https://www.epa.gov/ghgemissions/sources-greenhouse-gas-emissions> (accessed on 17 July 2022).
2. European Parliament News. EU Responses to Climate Change. 2022. Available online: <https://www.europarl.europa.eu/news/en/headlines/society/20180703STO07129/eu-responses-to-climate-change> (accessed on 17 July 2022).
3. Hesselgreaves, J.E.; Law, R.; Reay, D. *Compact Heat Exchangers: Selection, Design and Operation*; Butterworth-Heinemann: Oxford, UK, 2016.
4. Wang, L.; Sunden, B.; Manglik, R.M. *PHEs. Design, Applications and Performance*; WIT Press: Southampton, UK, 2007.

5. Abu-Khader, M.M. Plate heat exchangers: Recent advances. *Renew. Sustain. Energy Rev.* **2012**, *16*, 1883–1891. [[CrossRef](#)]
6. Zhang, J.; Zhu, X.; Mondejar, M.E.; Haglind, F. A review of heat transfer enhancement techniques in plate heat exchangers. *Renew. Sustain. Energy Rev.* **2019**, *101*, 305–328. [[CrossRef](#)]
7. Kumar, S.; Singh, S.K.; Sharma, D. A Comprehensive Review on Thermal Performance Enhancement of Plate Heat Exchanger. *Int. J. Thermophys.* **2022**, *43*, 109. [[CrossRef](#)]
8. Ma, Y.; Xie, G.; Hooman, K. Review of printed circuit heat exchangers and its applications in solar thermal energy. *Renew. Sustain. Energy Rev.* **2021**, *155*, 111933. [[CrossRef](#)]
9. Lalagi, G.; Nagaraj, P.B.; Veerabhadrapa Bidari, M.; Hegde, R.N. Influence of design of microchannel heat exchangers and use of nanofluids to improve the heat Transfer and Pressure drop characteristics: A review. *Int. J. Ambient. Energy* **2022**, *43*, 6849–6877. [[CrossRef](#)]
10. Martins, G.S.M.; Santiago, R.S.; Beckedorff, L.E.; Possamai, T.S.; Oba, R.; Oliveira, J.L.G.; de Oliveira, A.A.M.; Paiva, K.V. Structural analysis of gasketed plate heat exchangers. *Int. J. Press. Vessel. Pip.* **2022**, *197*, 104634. [[CrossRef](#)]
11. Dović, D.; Horvat, I.; Filipović, P. Impact of velocities and geometry on flow components and heat transfer in plate heat exchangers. *Appl. Therm. Eng.* **2021**, *197*, 117371. [[CrossRef](#)]
12. Hajabdollahi, H.; Naderi, M.; Adimi, S. A comparative study on the shell and tube and gasket-plate heat exchangers: The economic viewpoint. *Appl. Therm. Eng.* **2016**, *92*, 271–282. [[CrossRef](#)]
13. Wang, B.; Arsenyeva, O.; Zeng, M.; Klemeš, J.J.; Varbanov, P.S. An advanced Grid Diagram for heat exchanger network retrofit with detailed plate heat exchanger design. *Energy* **2022**, *248*, 123485. [[CrossRef](#)]
14. Arsenyeva, O.; Kapustenko, P.; Tovazhnyanskyy, L.; Khavin, G. The influence of plate corrugations geometry on plate heat exchanger performance in specified process conditions. *Energy* **2013**, *57*, 201–207. [[CrossRef](#)]
15. Kabil, B. Parameter Study of the Diagonal on a Gasketed Plate Heat Exchanger. Master's Dissertation, Division of Solid Mechanics, Lund University, Lund, Sweden, 2022.
16. AlfaLaval. Types of Gasketed Plate Heat Exchangers. 2022. Available online: <https://www.alfalaval.com/microsites/gphe/types/> (accessed on 24 June 2023).
17. de Souza, E.L.; de Souza Zanzi, M.; de Paiva, K.V.; Goes Oliveira, J.L.; Monteiro, A.S.; de Oliveira Barra, G.M.; Dutra, G.B. Evaluation of the aging of elastomeric acrylonitrile-butadiene rubber and ethylene-propylene-diene monomer gaskets used to seal plates heat exchanger. *Polym. Eng. Sci.* **2021**, *61*, 3001–3016. [[CrossRef](#)]
18. Zanzi, M.S.; de Souza, E.L.; Dutra, G.B.; Paiva, K.V.; Oliveira, J.L.G.; Cunha, T.V.; Monteiro, A.S. Service lifetime prediction of nitrile butadiene rubber gaskets used in plate heat exchangers. *J. Appl. Polym. Sci.* **2022**, *139*, 52523. [[CrossRef](#)]
19. Tian, C.; Zhang, D.-W.; Zhang, Q.; Zheng, Z.B.; Zhao, S.D. A drawing-flaring process of metal bushing ring without welding seam for plate heat exchanger. *Int. J. Adv. Manuf. Technol.* **2022**, *121*, 2539–2552. [[CrossRef](#)]
20. Trelleborg Sealing Solutions Plate Heat Exchanger Gaskets. 2022. Available online: <https://www.trelleborg.com/en/seals/products-and-solutions/engineered-molded-parts/plate-heat-exchanger-gaskets> (accessed on 24 June 2023).
21. Hashimoto, A.; Liu, S.B.; Shohji, I.; Kobayashi, T.; Hirohashi, J.; Wake, T.; Arai, S.; Kamakoshi, Y. Brazing of Stainless Steel Using Electrolytic Ni-P Plating Film and Investigation of Corrosion Behavior. *Mater. Sci. Forum* **2021**, *1016*, 522–527. [[CrossRef](#)]
22. AlfaLaval. Plate Heat Exchangers. 2022. Available online: <https://www.alfalaval.com/products/heat-transfer/plate-heat-exchangers/plate-heat-exchangers/> (accessed on 24 June 2023).
23. Tovazhnyanskyy, L.; Klemeš, J.J.; Kapustenko, P.; Arsenyeva, O.; Perevertaylenko, O.; Arsenyev, P. Optimal Design of Welded Plate Heat Exchanger for Ammonia Synthesis Column: An Experimental Study with Mathematical Optimisation. *Energies* **2020**, *13*, 2847. [[CrossRef](#)]
24. Freire, L.O.; de Andrade, D.A. On applicability of plate and shell heat exchangers for steam generation in naval PWR. *Nucl. Eng. Des.* **2014**, *280*, 619–627. [[CrossRef](#)]
25. Vahterus. PSHE Construction. 2022. Available online: <https://vahterus.com/technology/pshe-construction/> (accessed on 24 June 2023).
26. Martins, G.S.M.; da Silva, R.P.P.D.; Beckedorff, L.; Monteiro, A.S.; de Paiva, K.V.; Oliveira, J.L.G. Fatigue performance evaluation of plate and shell heat exchangers. *Int. J. Press. Vessel. Pip.* **2020**, *188*, 104237. [[CrossRef](#)]
27. Joybari, M.M.; Selvnas, H.; Sevault, A.; Hafner, A. Potentials and challenges for pillow-plate heat exchangers: State-of-the-art review. *Appl. Therm. Eng.* **2022**, *214*, 118739. [[CrossRef](#)]
28. Savostin, A.F.; Tikhonov, A.M. Investigation of the characteristics of the plate heating surfaces. *Therm. Eng.* **1970**, *17*, 113–117.
29. Rosenblad, G.; Kullendorff, A. Estimating heat transfer rates from mass transfer studies on plate heat exchanger surfaces. *Wärme-Und Stoffübertra.* **1975**, *8*, 187–191. [[CrossRef](#)]
30. Tovazhnyanskyy, L.L.; Kapustenko, P.A.; Tsibulnic, V.A. Heat Transfer and Hydraulic Resistance in Channels of Plate Heat Exchangers. *Energetika* **1980**, *9*, 123–125.
31. Focke, W.W.; Zachariades, J.; Olivier, I. The effect of the corrugation inclination angle on the thermohydraulic performance of plate heat exchangers. *Int. J. Heat Mass Transf.* **1985**, *28*, 1469–1479. [[CrossRef](#)]
32. Gaiser, G.; Kottke, V. Flow phenomena and local heat and mass transfer in corrugated passages. *Chem. Eng. Technol.* **1989**, *12*, 400–405. [[CrossRef](#)]
33. Heavner, R.L.; Kumar, H.; Wanniarachchi, A.S. *Performance of an Industrial Plate Heat Exchanger: Effect of Chevron Angle*; AIChE Symposium Series; American Institute of Chemical Engineers: New York, NY, USA, 1993; Volume 89, pp. 262–267.

34. Bogaert, R.; Bölcs, A. Global performance of a prototype brazed plate heat exchanger in a large Reynolds number range. *Exp. Heat Transf.* **1995**, *8*, 293–311. [[CrossRef](#)]
35. Muley, A.; Manglik, R.M.; Metwally, H.M. Enhanced heat transfer characteristics of viscous liquid flows in a chevron plate heat exchanger. *J. Heat Transf.* **1999**, *121*, 1011–1017. [[CrossRef](#)]
36. Muley, A.; Manglik, R.M. Experimental study of turbulent flow heat transfer and pressure drop in a plate heat exchanger with chevron plates. *ASME J. Heat Transf.* **1999**, *121*, 110–117. [[CrossRef](#)]
37. Zimmerer, C.; Gschwind, P.; Gaiser, G.; Kottke, V. Comparison of heat and mass transfer in different heat exchanger geometries with corrugated walls. *Exp. Therm. Fluid Sci.* **2002**, *26*, 269–273. [[CrossRef](#)]
38. Wang, Q.W.; Zhang, D.J.; Xie, G.N. Experimental study and genetic-algorithm-based correlation on pressure drop and heat transfer performances of a cross-corrugated primary surface heat exchanger. *Trans. ASME J. Heat Transf.* **2009**, *131*, 061802. [[CrossRef](#)]
39. Dović, D.; Palm, B.; Švaić, S. Generalized correlations for predicting heat transfer and pressure drop in plate heat exchanger channels of arbitrary geometry. *Int. J. Heat Mass Transf.* **2009**, *52*, 4553–4563. [[CrossRef](#)]
40. Khan, T.S.; Khan, M.S.; Chyu, M.C.; Ayub, Z.H. Experimental investigation of single phase convective heat transfer coefficient in a corrugated plate heat exchanger for multiple plate configurations. *Appl. Therm. Eng.* **2010**, *30*, 1058–1065. [[CrossRef](#)]
41. Gherasim, I.; Taws, M.; Galanis, N.; Nguyen, C.T. Heat transfer and fluid flow in a plate heat exchanger part I. Experimental investigation. *Int. J. Therm. Sci.* **2011**, *50*, 1492–1498. [[CrossRef](#)]
42. Shaji, K.; Das, S.K. Effect of plate characteristics on axial dispersion and heat transfer in plate heat exchangers. *Trans. ASME J. Heat Transf.* **2013**, *135*, 041801. [[CrossRef](#)]
43. Kılıç, B.; İpek, O. Experimental investigation of heat transfer and effectiveness in corrugated plate heat exchangers having different chevron angles. *Heat Mass Transf.* **2017**, *53*, 725–731. [[CrossRef](#)]
44. Kumar, B.; Singh, S.N. Study of pressure drop in single pass U-type plate heat exchanger. *Exp. Therm. Fluid Sci.* **2017**, *87*, 40–49. [[CrossRef](#)]
45. Yang, J.; Jacobi, A.; Liu, W. Heat transfer correlations for single-phase flow in plate heat exchangers based on experimental data. *Appl. Therm. Eng.* **2017**, *113*, 1547–1557. [[CrossRef](#)]
46. Khan, T.S.; Khan, M.S.; Ayub, Z.H. Single-phase flow pressure drop analysis in a plate heat exchanger. *Heat Transf. Eng.* **2017**, *38*, 256–264. [[CrossRef](#)]
47. Panday, N.K.; Singh, S.N. Experimental study of flow and thermal behaviour in single and multi-pass chevron-type plate heat exchangers. *Chem. Eng. Process.-Process Intensif.* **2022**, *171*, 108758. [[CrossRef](#)]
48. Lee, H.; Sadeghianjahromi, A.; Kuo, P.L.; Wang, C.C. Experimental investigation of the thermofluid characteristics of shell-and-plate heat exchangers. *Energies* **2020**, *13*, 5304. [[CrossRef](#)]
49. Kim, K.; Song, K.S.; Lee, G.; Chang, K.; Kim, Y. Single-Phase Heat Transfer Characteristics of Water in an Industrial Plate and Shell Heat Exchanger under High-Temperature Conditions. *Energies* **2021**, *14*, 6688. [[CrossRef](#)]
50. Beckedorff, L.; Martins, G.S.M.; de Paiva, K.V.; Oliveira, A.A., Jr.; Oliveira, J.L. Chevron Angle Effect on Plate and Shell Heat Exchangers Measured with Particle Tracking Velocimetry. *Heat Transf. Eng.* **2022**, *43*, 1885–1899. [[CrossRef](#)]
51. Martin, H. A theoretical approach to predict the performance of chevron-type plate heat exchangers. *Chem. Eng. Process. Process Intensif.* **1996**, *35*, 301–310. [[CrossRef](#)]
52. Dutta, O.Y.; Nageswara Rao, B. Investigations on the performance of chevron type plate heat exchangers. *Heat Mass Transf.* **2018**, *54*, 227–239. [[CrossRef](#)]
53. Arsenyeva, O.P.; Tovazhnyanskyy, L.L.; Kapustenko, P.O.; Khavin, G.L. The generalized correlation for friction factor in crisscross flow channels of plate heat exchangers. *Chem. Eng. Trans.* **2011**, *25*, 399–404. [[CrossRef](#)]
54. Churchill, S.W. Friction-factor equation spans all fluid-flow regimes. *Chem. Eng. USA* **1977**, *84*, 91–92.
55. Arsenyeva, O.P.; Tovazhnyanskyy, L.L.; Kapustenko, P.O.; Demirskiy, O.V. Heat transfer and friction factor in crisscross flow channels of plate-and-frame heat exchangers. *Theor. Found. Chem. Eng.* **2012**, *46*, 634–641. [[CrossRef](#)]
56. Delgado-García, D.C.; Picón-Núñez, M.; García-Castillo, J.L. Exploring Plate Heat Exchanger Design Options Using Generalised Correlations. *Chem. Eng. Trans.* **2022**, *94*, 61–66.
57. Gusew, S.; Stuke, R. Pressure Drop in Plate Heat Exchangers for Single-Phase Convection in Turbulent Flow Regime: Experiment and Theory. *Int. J. Chem. Eng.* **2019**, *2019*, 3693657. [[CrossRef](#)]
58. Gusew, S.; Stuke, R. Plate heat exchangers: Calculation of pressure drop for single phase convection in turbulent flow regime. *Heat Mass Transf.* **2022**, *58*, 419–430. [[CrossRef](#)]
59. Stogiannis, I.A.; Paras, S.V.; Arsenyeva, O.P.; Kapustenko, P.O. CFD modelling of hydrodynamics and heat transfer in channels of a PHE. *Chem. Eng. Trans.* **2013**, *35*, 1285–1290. [[CrossRef](#)]
60. Klemeš, J.J.; Arsenyeva, O.; Kapustenko, P.; Tovazhnyanskyy, L. *Compact Heat Exchangers for Energy Transfer Intensification: Low Grade Heat and Fouling Mitigation*; CRC Press: Boca Raton, FL, USA, 2015.
61. Arsenyeva, O.P.; Tovazhnyanskyy, L.L.; Kapustenko, P.O.; Demirskiy, O.V. Generalised semi-empirical correlation for heat transfer in channels of plate heat exchanger. *Appl. Therm. Eng.* **2014**, *70*, 1208–1215. [[CrossRef](#)]
62. Wehling, P.; Younis, B.A.; Weigand, B. Heat transfer enhancement in a ribbed channel: Development of turbulence closures. *Int. J. Heat Mass Transf.* **2014**, *76*, 509–522. [[CrossRef](#)]

63. Amano, R.S. Turbulent heat transfer in a channel with two right-angle bends. *Int. J. Heat Mass Transf.* **1985**, *28*, 2177–2179. [[CrossRef](#)]
64. Ciofalo, M.; Stasiak, J.; Collins, M.W. Investigation of flow and heat transfer in corrugated passages—II. Numerical simulations. *Int. J. Heat Mass Transf.* **1996**, *39*, 165–192. [[CrossRef](#)]
65. Blomerius, H.; Mitra, N.K. Numerical investigation of convective heat transfer and pressure drop in wavy ducts. *Numer. Heat Transf. Part A Appl.* **2000**, *37*, 37–54. [[CrossRef](#)]
66. Croce, G.; d’Agaro, P. Numerical analysis of forced convection in plate and frame heat exchangers. *Int. J. Numer. Methods Heat Fluid Flow* **2002**, *12*, 756–771. [[CrossRef](#)]
67. Metwally, H.M.; Manglik, R.M. Enhanced heat transfer due to curvature-induced lateral vortices in laminar flows in sinusoidal corrugated-plate channels. *Int. J. Heat Mass Transf.* **2004**, *47*, 2283–2292. [[CrossRef](#)]
68. Zhang, L.Z. Numerical study of periodically fully developed flow and heat transfer in cross-corrugated triangular channels in transitional flow regime. *Numer. Heat Transf. Part A Appl.* **2005**, *48*, 387–405. [[CrossRef](#)]
69. Ansys Fluids. Computational Fluid Dynamics (CFD) Simulation Software. Available online: <https://www.ansys.com/products/fluids> (accessed on 20 September 2022).
70. Islamoglu, Y.; Parmaksizoglu, C. Numerical investigation of convective heat transfer and pressure drop in a corrugated heat exchanger channel. *Appl. Therm. Eng.* **2004**, *24*, 141–147. [[CrossRef](#)]
71. Galeazzo, F.C.; Miura, R.Y.; Gut, J.A.; Tadini, C.C. Experimental and numerical heat transfer in a plate heat exchanger. *Chem. Eng. Sci.* **2006**, *61*, 7133–7138. [[CrossRef](#)]
72. Kanaris, A.G.; Mouza, A.A.; Paras, S.V. Flow and heat transfer in narrow channels with corrugated walls: A CFD code application. *Chem. Eng. Res. Des.* **2005**, *83*, 460–468. [[CrossRef](#)]
73. Jain, S.; Joshi, A.; Bansal, P.K. A new approach to numerical simulation of small sized plate heat exchangers with chevron plates. *ASME J. Heat Transf.* **2007**, *129*, 291–297. [[CrossRef](#)]
74. Tsai, Y.C.; Liu, F.B.; Shen, P.T. Investigations of the pressure drop and flow distribution in a chevron-type plate heat exchanger. *Int. Commun. Heat Mass Transf.* **2009**, *36*, 574–578. [[CrossRef](#)]
75. Zhang, L.; Che, D. Influence of corrugation profile on the thermohydraulic performance of cross-corrugated plates. *Numer. Heat Transf. Part A Appl.* **2011**, *59*, 267–296. [[CrossRef](#)]
76. Zhao, Y.; Wu, Y.; Cheng, H.; Zhu, G. Numerical simulation of corrugated inclination angle on the performance of plate heat exchanger. In Proceedings of the 2014 International Conference on Mechatronics, Electronic, Industrial and Control Engineering (MEIC-14), Shenyang, China, 17–19 November 2014; Atlantis Press: Amsterdam, The Netherlands, 2014; pp. 1250–1253.
77. Sarraf, K.; Launay, S.; Tadrist, L. Complex 3D-flow analysis and corrugation angle effect in plate heat exchangers. *Int. J. Therm. Sci.* **2015**, *94*, 126–138. [[CrossRef](#)]
78. Zhao, Y.H.; Wu, Y.F.; Cheng, H.J.; Zhu, G.L. Numerical simulation of corrugated depth on the performance of plate heat exchanger. In *Advanced Materials Research*; Trans Tech Publications Ltd.: Stafa-Zurich, Switzerland, 2014; Volume 860, pp. 696–699.
79. Vafajoo, L.; Moradifar, K.; Hosseini, S.M.; Salman, B.H. Mathematical modelling of turbulent flow for flue gas–air Chevron type plate heat exchangers. *Int. J. Heat Mass Transf.* **2016**, *97*, 596–602. [[CrossRef](#)]
80. Lee, J.; Lee, K.S. Flow characteristics and thermal performance in chevron type plate heat exchangers. *Int. J. Heat Mass Transf.* **2014**, *78*, 699–706. [[CrossRef](#)]
81. Hu, X.; Haglind, F. Relationship between inclination angle and friction factor of chevron-type plate heat exchangers. *Int. J. Heat Mass Transf.* **2020**, *162*, 120370.
82. Li, W.; Hrnjak, P. Single-phase flow distribution in plate heat exchangers: Experiments and models. *Int. J. Refrig.* **2021**, *126*, 45–56. [[CrossRef](#)]
83. Sadeghianjahromi, A.; Jafari, A.; Wang, C.C. Numerical investigation of the effect of chevron angle on thermofluids characteristics of non-mixed and mixed brazed plate heat exchangers with experimental validation. *Int. J. Heat Mass Transf.* **2022**, *184*, 122278. [[CrossRef](#)]
84. Jafari, A.; Sadeghianjahromi, A.; Wang, C.C. Experimental and numerical investigation of brazed plate heat exchangers—A new approach. *Appl. Therm. Eng.* **2022**, *200*, 117694. [[CrossRef](#)]
85. Yu, J.; Qiu, H.; Jiao, Y.; Tian, Y.; Meng, Y.; Wang, W.; Min, H.; Li, X. Numerical prediction of heat transfer performance of plate heat exchanger based on experimental data assimilation to calibrate turbulence model constants. *Therm. Sci. Eng. Prog.* **2022**, *34*, 101433. [[CrossRef](#)]
86. Luan, H.B.; Kuang, J.P.; Cao, Z.; Wu, Z.; Tao, W.Q.; Sundén, B. CFD analysis of two types of welded plate heat exchangers. *Numer. Heat Transf. Part A Appl.* **2017**, *71*, 250–269. [[CrossRef](#)]
87. Durmuş, A.; Benli, H.; Kurtbaş, İ.; Gül, H. Investigation of heat transfer and pressure drop in plate heat exchangers having different surface profiles. *Int. J. Heat Mass Transf.* **2009**, *52*, 1451–1457. [[CrossRef](#)]
88. Luan, Z.J.; Zhang, G.M.; Tian, M.C.; Fan, M.X. Flow resistance and heat transfer characteristics of a new-type plate heat exchanger. *J. Hydrodyn.* **2008**, *20*, 524–529. [[CrossRef](#)]
89. Kanaris, A.G.; Mouza, A.A.; Paras, S.V. Optimal design of a plate heat exchanger with undulated surfaces. *Int. J. Therm. Sci.* **2009**, *48*, 1184–1195. [[CrossRef](#)]

90. Han, W.; Saleh, K.; Aute, V.; Ding, G.; Hwang, Y.; Radermacher, R. Numerical simulation and optimization of single-phase turbulent flow in chevron-type plate heat exchanger with sinusoidal corrugations. *HVACR Res.* **2011**, *17*, 186–197. [[CrossRef](#)]
91. Kan, M.; Ipek, O.; Gurel, B. Plate heat exchangers as a compact design and optimization of different channel angles. *Acta Phys. Pol. A* **2015**, *12*, 49–52. [[CrossRef](#)]
92. Kim, M.; Baik, Y.J.; Park, S.R.; Ra, H.S.; Lim, H. Experimental study on corrugated cross-flow air-cooled plate heat exchangers. *Exp. Therm. Fluid Sci.* **2010**, *34*, 1265–1272. [[CrossRef](#)]
93. Doo, J.H.; Ha, M.Y.; Min, J.K.; Stieger, R.; Rolt, A.; Son, C. An investigation of cross-corrugated heat exchanger primary surfaces for advanced intercooled-cycle aero engines (Part-I: Novel geometry of primary surface). *Int. J. Heat Mass Transf.* **2012**, *55*, 5256–5267. [[CrossRef](#)]
94. Doo, J.H.; Ha, M.Y.; Min, J.K.; Stieger, R.; Rolt, A.; Son, C. An investigation of cross-corrugated heat exchanger primary surfaces for advanced intercooled-cycle aero engines (Part-II: Design optimization of primary surface). *Int. J. Heat Mass Transf.* **2013**, *61*, 138–148. [[CrossRef](#)]
95. Du, W.; Wang, F.; Xin, G.; Zhang, S.; Cheng, L. Numerical Investigation and Thermodynamic Analysis on a Novel Regular Hexagonal Plate Heat Exchanger. In Proceedings of the 2010 14th International Heat Transfer Conference, Washington, DC, USA, 8–13 August 2010; Volume 49392, pp. 257–263.
96. Song, J.; Wang, F.; Cheng, L. Experimental study and analysis of a novel multi-media plate heat exchanger. *Sci. China Technol. Sci.* **2012**, *55*, 2157–2162. [[CrossRef](#)]
97. Yuan, Z.; Wu, L.; Yuan, Z.; Li, H. Shape optimization of welded plate heat exchangers based on grey correlation theory. *Appl. Therm. Eng.* **2017**, *123*, 761–769.
98. Javed, S.A.; Mahmoudi, A.; Khan, A.M.; Javed, S.; Liu, S. A critical review: Shape optimization of welded plate heat exchangers based on grey correlation theory. *Appl. Therm. Eng.* **2018**, *144*, 593–599. [[CrossRef](#)]
99. El-Said, E.M.; Elshamy, S.M.; Hegazi, A.A. Experimental investigation on thermo-hydraulic performance of a helical plate heat exchanger. *Exp. Heat Transf.* **2022**, *36*, 453–472. [[CrossRef](#)]
100. Al Zahrani, S.; Islam, M.S.; Saha, S.C. Heat transfer enhancement investigation in a novel flat plate heat exchanger. *Int. J. Therm. Sci.* **2021**, *161*, 106763. [[CrossRef](#)]
101. Al Zahrani, S.; Islam, M.S.; Saha, S.C. Heat transfer enhancement of modified flat plate heat exchanger. *Appl. Therm. Eng.* **2021**, *186*, 116533. [[CrossRef](#)]
102. Zhang, Y.; Jiang, C.; Yang, Z.; Zhang, Y.; Bai, B. Numerical study on heat transfer enhancement in capsule-type plate heat exchangers. *Appl. Therm. Eng.* **2016**, *108*, 1237–1242. [[CrossRef](#)]
103. Alqutub, A.M.; Linjawi, M.T.; Alrawi, I.M. Performance study of a dimpled-protruded air-to-air plate heat exchanger. In *ASME Power Conference*; American Society of Mechanical Engineers: New York, NY, USA, 2015; Volume 56604, p. V001T04A006.
104. Ji, C.; Wu, L.; Li, J.; Wang, X. Experimental research on heat transfer characteristics of Dimple plate heat exchanger. In Proceedings of the 5th International Conference on Advanced Design and Manufacturing Engineering (979–983), Shenzhen, China, 19–20 September 2015; Atlantis Press: Paris, France, 2015.
105. Soman, D.P.; Karthika, S.; Kalaichelvi, P.; Radhakrishnan, T.K. Experimental study of turbulent forced convection heat transfer and friction factor in dimpled plate heat exchanger. *Appl. Therm. Eng.* **2019**, *162*, 114254. [[CrossRef](#)]
106. Khail, A.A.; Erişen, A. Improvement of Plate Heat Exchanger Performance Using a New Plate Geometry. *Arab. J. Sci. Eng.* **2021**, *46*, 2877–2889. [[CrossRef](#)]
107. Ma, Q.; Yang, Y.; Zuo, Y. Thermal performance optimization of heat exchanger with mixed cross-corrugated sinusoidal plate channels. *Appl. Therm. Eng.* **2021**, *195*, 117138. [[CrossRef](#)]
108. Mohebbi, S.; Veysi, F. Numerical investigation of small plate heat exchangers performance having different surface profiles. *Appl. Therm. Eng.* **2021**, *188*, 116616. [[CrossRef](#)]
109. Yu, C.; Xue, X.; Shi, K.; Shao, M. Optimization of thermal and flow characteristics of plate heat exchanger with variable structure parameter. *J. Therm. Anal. Calorim.* **2022**, *147*, 12617–12629. [[CrossRef](#)]
110. Zhang, J.; Zhou, N.; Zhang, G.; Tian, M. Numerical and experimental studies of flow and heat transfer characteristics in a plate heat exchanger with multi-chevron corrugate furrows. *Numer. Heat Transf. Part A Appl.* **2022**, *84*, 71–82. [[CrossRef](#)]
111. Wajs, J.; Mikielwicz, D. Effect of surface roughness on thermal-hydraulic characteristics of plate heat exchanger. In *Key Engineering Materials*; Trans Tech Publications Ltd.: Stafa-Zurich, Switzerland, 2014; Volume 597, pp. 63–74.
112. Wajs, J.; Mikielwicz, D. Influence of metallic porous microlayer on pressure drop and heat transfer of stainless steel plate heat exchanger. *Appl. Therm. Eng.* **2016**, *93*, 1337–1346. [[CrossRef](#)]
113. Nilpueng, K.; Wongwises, S. Experimental study of single-phase heat transfer and pressure drop inside a plate heat exchanger with a rough surface. *Exp. Therm. Fluid Sci.* **2015**, *68*, 268–275. [[CrossRef](#)]
114. Nilpueng, K.; Keawkamrop, T.; Ahn, H.S.; Wongwises, S. Effect of chevron angle and surface roughness on thermal performance of single-phase water flow inside a plate heat exchanger. *Int. Commun. Heat Mass Transf.* **2018**, *91*, 201–209. [[CrossRef](#)]
115. Nguyen, D.H.; Kim, K.M.; Shim, G.H.; Kim, J.H.; Lee, C.H.; Lim, S.T.; Ahn, H.S. Experimental study on the thermal-hydraulic performance of modified chevron plate heat exchanger by electrochemical etching method. *Int. J. Heat Mass Transf.* **2020**, *155*, 119857. [[CrossRef](#)]

116. Nguyen, D.H.; Kim, K.M.; Vo, T.T.N.; Shim, G.H.; Kim, J.H.; Ahn, H.S. Improvement of thermal-hydraulic performance of plate heat exchanger by electroless nickel, copper and silver plating. *Case Stud. Therm. Eng.* **2021**, *23*, 100797. [CrossRef]
117. Das, S.K.; Choi, S.U.; Patel, H.E. Heat transfer in nanofluids—A review. *Heat Transf. Eng.* **2006**, *27*, 3–19. [CrossRef]
118. Kumar, V.; Tiwari, A.K.; Ghosh, S.K. Application of nanofluids in plate heat exchanger: A review. *Energy Convers. Manag.* **2015**, *105*, 1017–1036. [CrossRef]
119. Pandya, N.S.; Shah, H.; Molana, M.; Tiwari, A.K. Heat transfer enhancement with nanofluids in plate heat exchangers: A comprehensive review. *Eur. J. Mech.-B/Fluids* **2020**, *81*, 173–190. [CrossRef]
120. Gupta, S.K.; Gupta, S.; Gupta, T.; Raghav, A.; Singh, A. A review on recent advances and applications of nanofluids in plate heat exchanger. *Mater. Today Proc.* **2021**, *44*, 229–241. [CrossRef]
121. Ajeeb, W.; Murshed, S.S. Nanofluids in compact heat exchangers for thermal applications: A State-of-the-art review. *Therm. Sci. Eng. Prog.* **2022**, *30*, 101276. [CrossRef]
122. Mousa, M.H.; Miljkovic, N.; Nawaz, K. Review of heat transfer enhancement techniques for single phase flows. *Renew. Sustain. Energy Rev.* **2021**, *137*, 110566. [CrossRef]
123. Bhattacharyya, S.; Vishwakarma, D.K.; Srinivasan, A.; Soni, M.K.; Goel, V.; Sharifpur, M.; Ahmadi, M.H.; Issakhov, A.; Meyer, J. Thermal performance enhancement in heat exchangers using active and passive techniques: A detailed review. *J. Therm. Anal. Calorim.* **2022**, *147*, 9229–9281. [CrossRef]
124. Thapa, S.; Samir, S.; Kumar, K.; Singh, S. A review study on the active methods of heat transfer enhancement in heat exchangers using electroactive and magnetic materials. *Mater. Today Proc.* **2021**, *45*, 4942–4947. [CrossRef]
125. Diaconu, B.M.; Cruceru, M.; Angheliescu, L. A critical review on heat transfer enhancement techniques in latent heat storage systems based on phase change materials. Passive and active techniques, system designs and optimization. *J. Energy Storage* **2023**, *61*, 106830. [CrossRef]
126. Dehbani, M.; Rahimi, M.; Rahimi, Z. A review on convective heat transfer enhancement using ultrasound. *Appl. Therm. Eng.* **2022**, *208*, 118273. [CrossRef]
127. Alikhan, A.H.; Maghrebi, M.J. Experimental investigation on frequency pulsation effects on a single pass plate heat exchanger performance. *Heat Transf.* **2022**, *51*, 2688–2701. [CrossRef]
128. Sarafraz, M.M.; Nikkhah, V.; Madani, S.A.; Jafarian, M.; Hormozi, F. Low-frequency vibration for fouling mitigation and intensification of thermal performance of a plate heat exchanger working with CuO/water nanofluid. *Appl. Therm. Eng.* **2017**, *121*, 388–399. [CrossRef]
129. Guo, C.; Gao, M.; Wei, W.; Liu, Z.; Guo, L. Influence of frequency and intensity of bilateral audible sound waves on heat transfer performance of air-to-air heat exchange systems. *Int. J. Heat Mass Transf.* **2023**, *203*, 123797. [CrossRef]
130. Hotrum, N.E.; de Jong, P.; Akkerman, J.C.; Fox, M.B. Pilot scale ultrasound enabled plate heat exchanger—Its design and potential to prevent biofouling. *J. Food Eng.* **2015**, *153*, 81–88. [CrossRef]
131. Vasyliiev, G.S.; Novosad, A.A.; Pidburtnyi, M.O.; Chyhryn, O.M. Influence of ultrasound vibrations on the corrosion resistance of heat-exchange plates made of AISI 316 steel. *Mater. Sci.* **2019**, *54*, 913–919. [CrossRef]
132. Tiwari, J.; Kim, K.; Zhang, M.; Yeom, T. Experimental study on convection heat transfer enhancement of channel-flow with piezoelectric fan. *Heat Transf. Eng.* **2023**, *44*, 65–86. [CrossRef]
133. Vahterus. Plate & Shell Heat Exchangers for Every Application. 2023. Available online: <https://vahterus.com/applications/> (accessed on 24 June 2023).
134. Lamb, B.R. Plate heat exchangers—A low-cost route to heat recovery. *J. Heat Recovery Syst.* **1982**, *2*, 247–255. [CrossRef]
135. Grillot, J.M. Compact heat exchangers liquid-side fouling. *Appl. Therm. Eng.* **1997**, *17*, 717–726. [CrossRef]
136. Reppich, M. Use of high performance plate heat exchangers in chemical and process industries. *Int. J. Therm. Sci.* **1999**, *38*, 999–1008. [CrossRef]
137. Lozano, A.; Barreras, F.; Fueyo, N.; Santodomingo, S. The flow in an oil/water plate heat exchanger for the automotive industry. *Appl. Therm. Eng.* **2008**, *28*, 1109–1117. [CrossRef]
138. Kandilli, C.; Koclu, A. Assessment of the optimum operation conditions of a plate heat exchanger for waste heat recovery in textile industry. *Renew. Sustain. Energy Rev.* **2011**, *15*, 4424–4431. [CrossRef]
139. Kapustenko, P.; Boldyryev, S.; Arsenyeva, O.; Khavin, G. The use of plate heat exchangers to improve energy efficiency in phosphoric acid production. *J. Clean. Prod.* **2009**, *17*, 951–958. [CrossRef]
140. Andersson, E.; Quah, J.; Polley, G.T. Experience in application of Compabloc heat exchangers in refinery pre-heat trains. In Proceedings of the International Conference on Heat Exchanger Fouling and Cleaning VIII-2009, Schladming, Austria, 14–19 June 2009; Muller-Steinhagen, H., Malayeri, M.R., Watkinson, A.P., Eds.; pp. 39–43.
141. Polyvianchuk, A.; Semenenko, R.; Kapustenko, P.; Klemeš, J.J.; Arsenyeva, O. The efficiency of innovative technologies for transition to 4th generation of district heating systems in Ukraine. *Energy* **2023**, *263*, 125876. [CrossRef]
142. Klemes, J.J. (Ed.) *Handbook of Process Integration (PI): Minimisation of Energy and Water Use, Waste and Emissions*; Woodhead Publishing: Oxford, UK, 2022.
143. Kapustenko, P.O.; Ulyev, L.M.; Boldyryev, S.A.; Garev, A.O. Integration of a heat pump into the heat supply system of a cheese production plant. *Energy* **2008**, *33*, 882–889. [CrossRef]

144. Tovazhnyansky, L.; Kapustenko, P.; Ulyev, L.; Boldyryev, S.; Arsenyeva, O. Process integration of sodium hypophosphite production. *Appl. Therm. Eng.* **2010**, *30*, 2306–2314. [[CrossRef](#)]
145. Perevertaylenko, O.Y.; Gariev, A.O.; Damartzis, T.; Tovazhnyansky, L.L.; Kapustenko, P.O.; Arsenyeva, O.P. Searches of cost effective ways for amine absorption unit design in CO₂ post-combustion capture process. *Energy* **2015**, *90*, 105–112. [[CrossRef](#)]
146. Kapustenko, P.; Arsenyeva, O.; Fedorenko, O.; Kusakov, S. Integration of low-grade heat from exhaust gases into energy system of the enterprise. *Clean Technol. Environ. Policy* **2022**, *24*, 67–76. [[CrossRef](#)]
147. Li, N.; Klemeš, J.J.; Sunden, B.; Wu, Z.; Wang, Q.; Zeng, M. Heat exchanger network synthesis considering detailed thermal-hydraulic performance: Methods and perspectives. *Renew. Sustain. Energy Rev.* **2022**, *168*, 112810. [[CrossRef](#)]

Disclaimer/Publisher's Note: The statements, opinions and data contained in all publications are solely those of the individual author(s) and contributor(s) and not of MDPI and/or the editor(s). MDPI and/or the editor(s) disclaim responsibility for any injury to people or property resulting from any ideas, methods, instructions or products referred to in the content.